Measurements of diffractive physics and soft QCD at ATLAS

28th International Workshop on Deep Inelastic Scattering
14 April 2021

Jesse Liu (University of Chicago)
On behalf of the ATLAS Collaboration

ATLAS EXPERIMENT

THE UNIVERSITY OF CHICAGO

INTERCONNECTED PROBES OF SOFT QCD & DIFFRACTION

Fig: ATLAS-PHOTO-2016-009-4

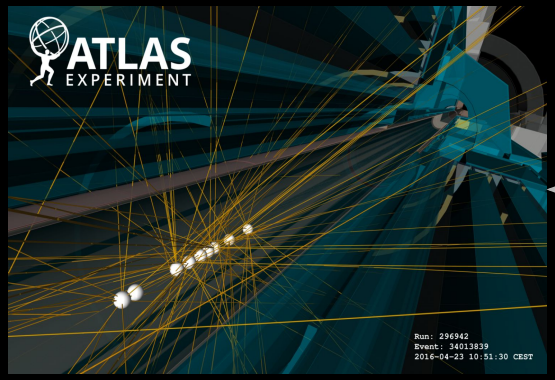

$$-\frac{1}{4}F^a_{\mu\nu}F_a^{\mu\nu}$$

$$+\,\mathrm{i}\bar{\psi}\gamma^\mu D_\mu\psi$$

Fig: A. Chantelauze, S. Staffi, L. Bret

Laboratory
Colliders and detectors

Calculation
Models and generators

Nature
Cosmic ray observatories

Why is this the only known force that confines?
Does it accidentally or dynamically conserve CP?
How can we better model cosmic-ray air showers?
How do long-range nonperturbative dynamics emerge?
What measurements improve MC precision to probe new physics?

The strong force is still fundamentally mysterious

Foundational and practical open questions endure

Retrospective: diverse ATLAS sQCD science in 2010s

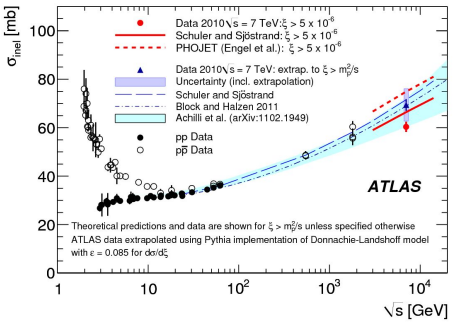

Total pp σ(inel)
Nat Comm 2 (2011) 463
PRL 117 (2016) 182002

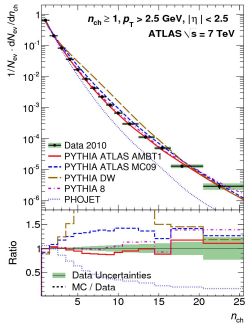

Charged particles
NJP 13 (2010) 053033
PLB 758 (2016) 67

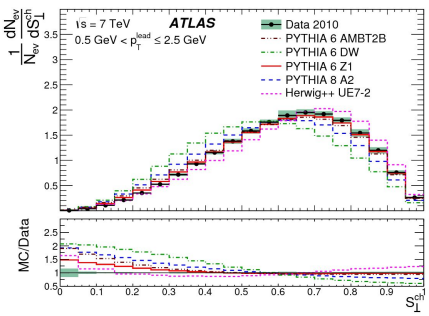

Event shapes
PRD 83 (2011) 052003
PRD 88 (2013) 032004

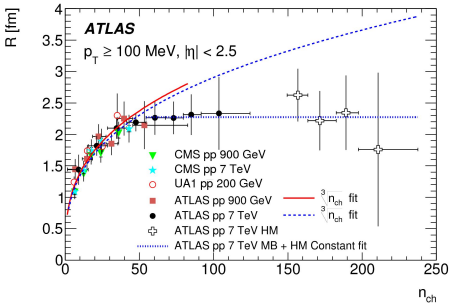

Long-range dynamics
EPJC 75 (2015) 466
PRD 96 (2017) 092008

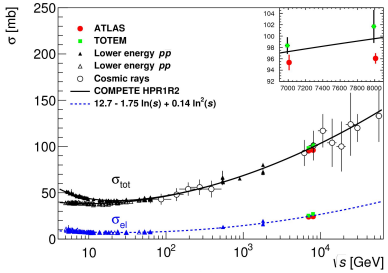

ALFA σ(el) and σ(tot)
Nucl.Phys.B 889 (2014) 486-548
PLB 761 (2016) 158

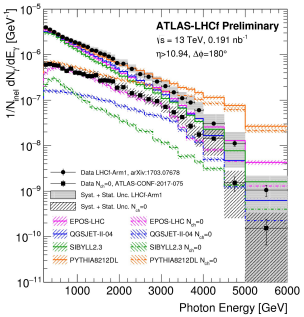

ATLAS+LHCf spectra
PHYS-PUB-2015-038
CONF-2017-075

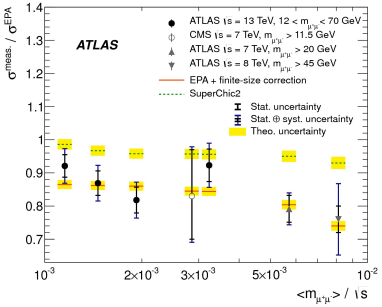

Exclusive production
PRD 94 (2016) 032011
PLB 77 (2018) 303

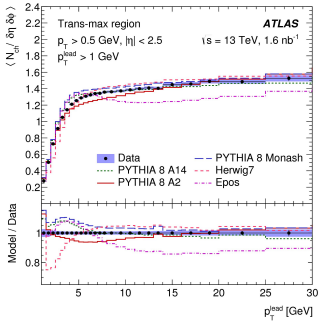

Underlying event
JHEP 03 (2017) 157
EPJC 79 (2019) 666

ATLAS opened rich programme of landmark measurements in past decade
Often requires dedicated detectors, special runs, nonstandard techniques
Advancing nonperturbative QCD, modelling accuracy & cosmic ray science

Non-exhaustive references above: please see full list of ATLAS SM Results

Today: highlight two recent publications

pp → p+X: single diffraction with ALFA (low-μ dataset)

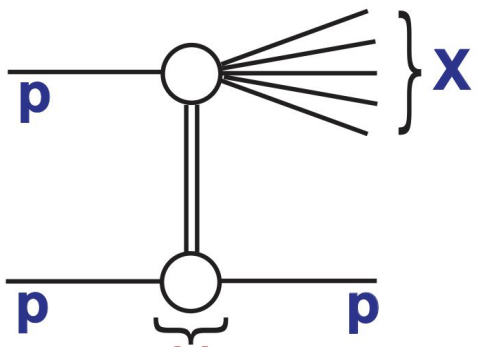

JHEP

Published for SISSA by Springer

Received: *November 4, 2019*
Accepted: *January 23, 2020*
Published: *February 6, 2020*

JHEP 02 (2020) 042

Measurement of differential cross sections for single diffractive dissociation in $\sqrt{s} = 8$ TeV pp collisions using the ATLAS ALFA spectrometer

pp → p(γγ → ℓℓ)p$^{(*)}$: photon fusion with AFP (high-μ dataset)

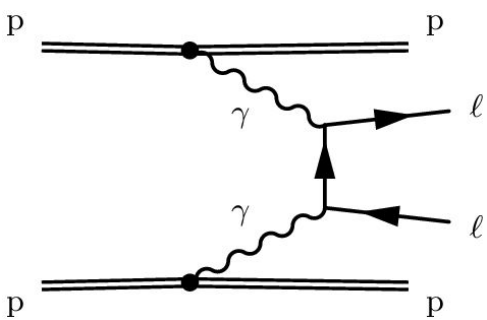

PHYSICAL REVIEW LETTERS **125,** 261801 (2020)

PRL 125 (2020) 261801

Observation and Measurement of Forward Proton Scattering in Association with Lepton Pairs Produced via the Photon Fusion Mechanism at ATLAS

G. Aad *et al.*[*]
(ATLAS Collaboration)

(Received 2 October 2020; revised 30 October 2020; accepted 23 November 2020; published 23 December 2020)

Two complementary results demonstrating forward proton spectrometry in ATLAS

FORWARD DETECTORS

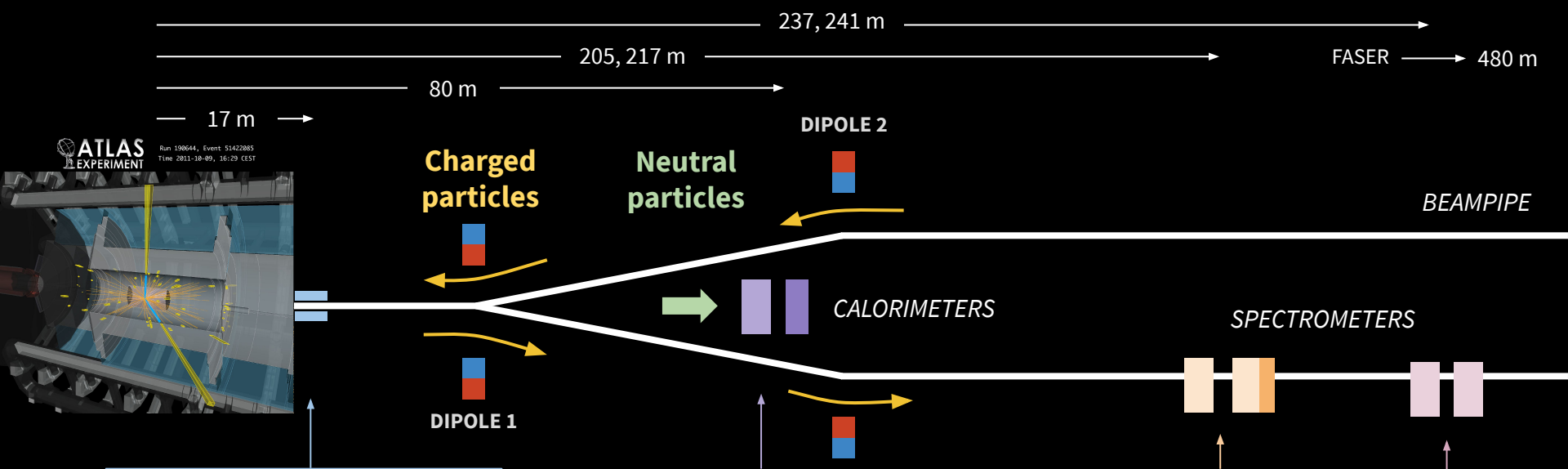

LUCID

Luminosity Cherenkov Integrating Detector

$5.6 < |\eta| < 5.9$

For luminosity measurement

LHCf

LHC Forward

ZDC

Zero Degree Calorimeter

Low-μ, $|\eta| > 8.0$

For cosmic-ray & heavy-ion physics

AFP

ATLAS Forward Proton
Low & high μ
$0.02 < \xi < 0.12$

ALFA

Absolute Luminosity For ATLAS
Low-μ, $0 < \xi < 0.2$
$10.6 < |\eta| < 13.5$

TODAY'S FOCUS

ALFA analysis: signal and event topology

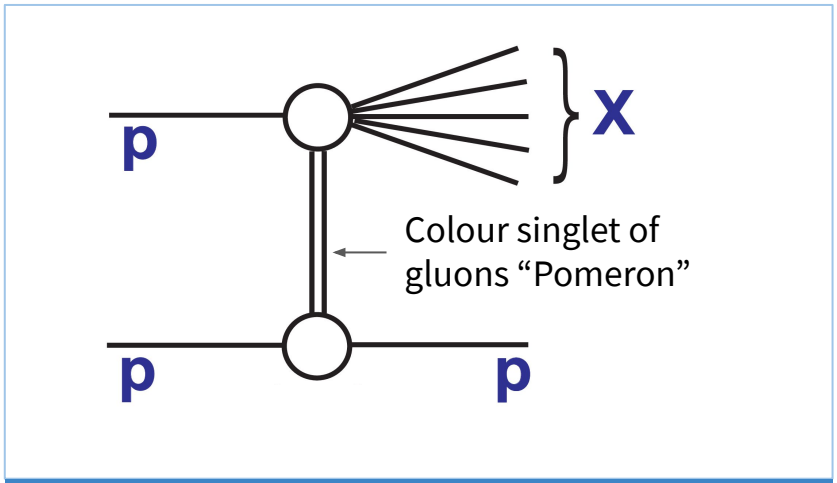

Signal: single diffractive dissociation (SD)

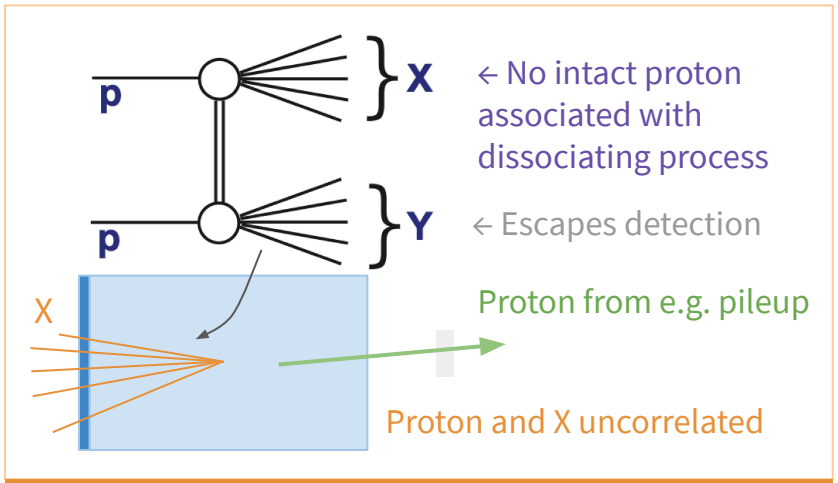

Background: dominated by overlay

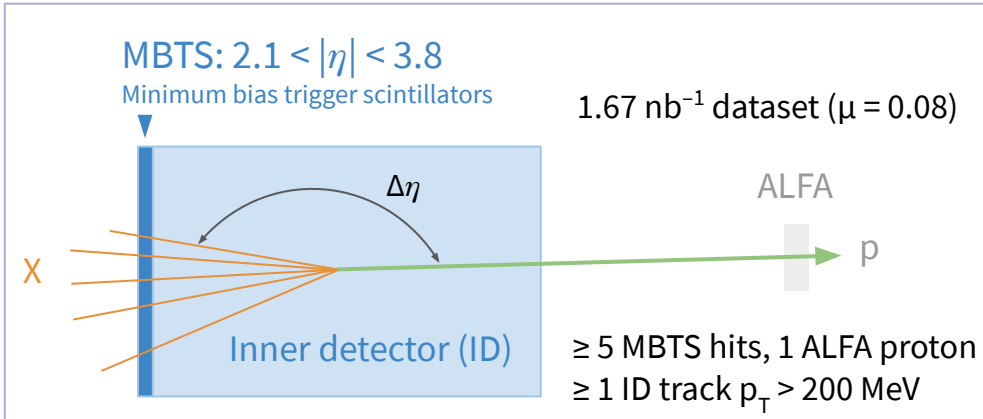

1.67 nb^{-1} dataset ($\mu = 0.08$)

≥ 5 MBTS hits, 1 ALFA proton
≥ 1 ID track p_T > 200 MeV

↑ Cartoon of signal event topology

→ Pb+Pb event illustrates what rapidity gaps look like in ATLAS

Event Displays

JHEP 02 (2020) 042

Detector-level distributions: nominal & control regions

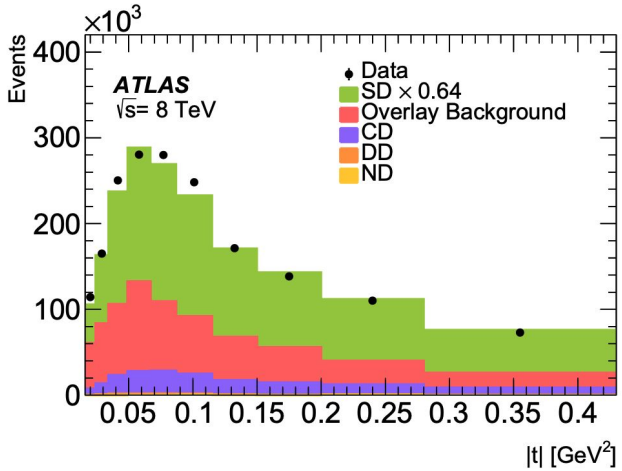

(c) Nominal Sample

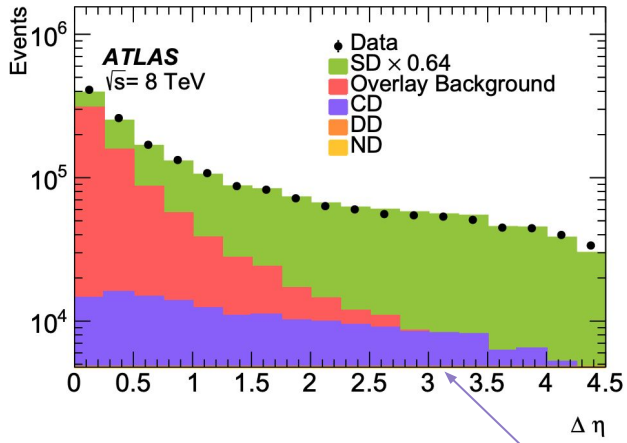

(d) Nominal Sample

← Nominal regions where backgrounds subtracted and measurement performed

↓ These two data samples are control regions ↓

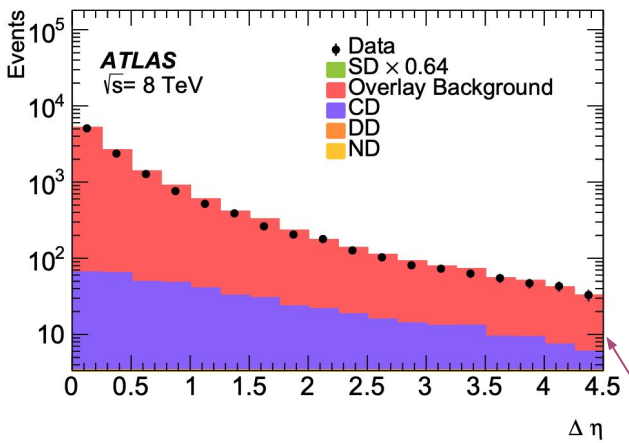

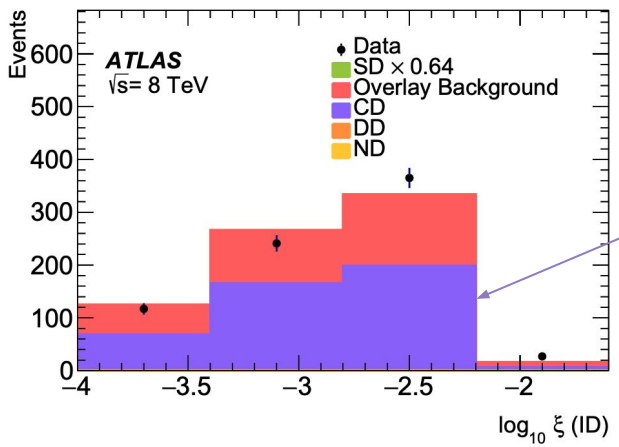

Central diffraction (CD)

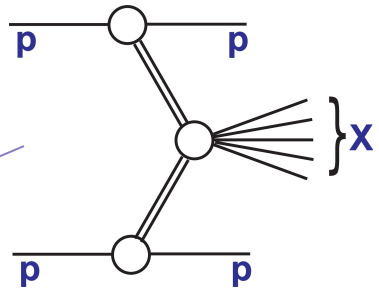

Subdominant bkg estimated from MC

Data-driven estimate of **overlay backgrounds**

JHEP 02 (2020) 042

Measurements: cross-section vs rapidity gap

Distribution	$\sigma_{SD}^{\text{fiducial}(\xi,t)}$ [mb]	$\sigma_{SD}^{t\text{-extrap}}$ [mb]
Data	1.59 ± 0.13	1.88 ± 0.15
PYTHIA8 A2 (Schuler–Sjöstrand)	3.69	4.35
PYTHIA8 A3 (Donnachie–Landshoff)	2.52	2.98
HERWIG7	4.96	6.11

← **Inclusive cross-section measurements vs predictions**

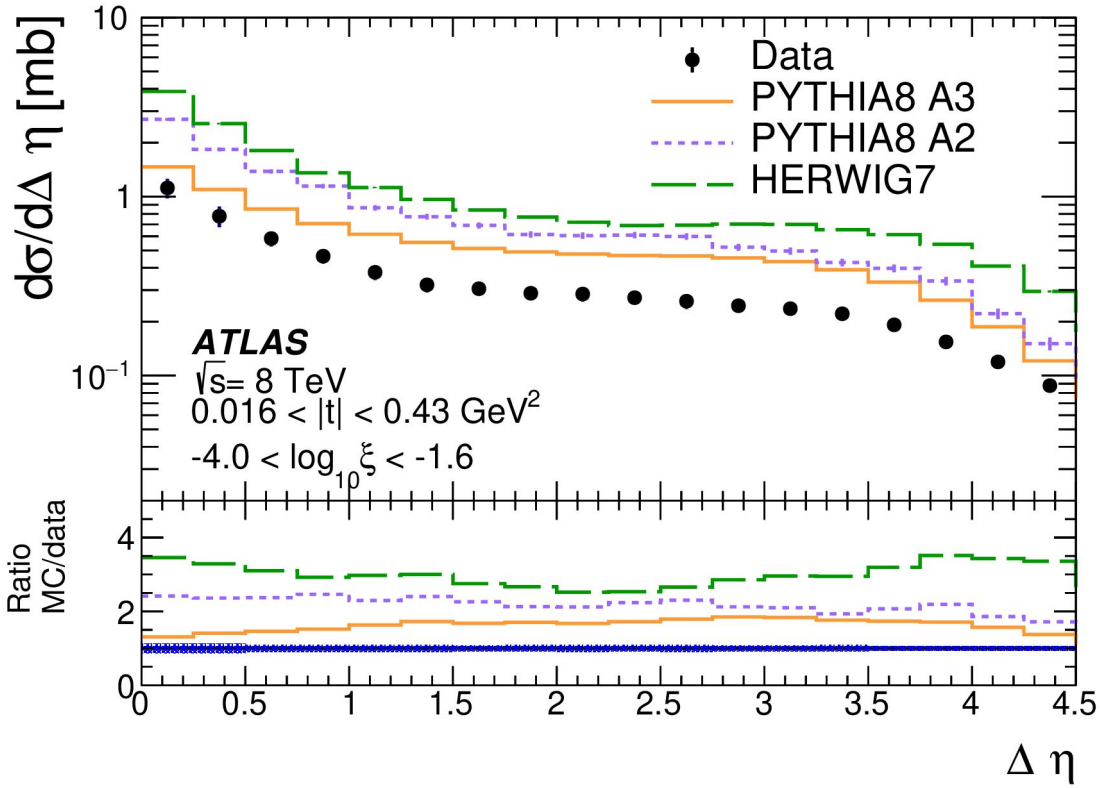

← **Rapidity gap size $\Delta\eta$**

Significant normalisation overpredictions and mild shape mismodelling vs MC

JHEP 02 (2020) 042

Measurements: exponential fit & momentum transfer

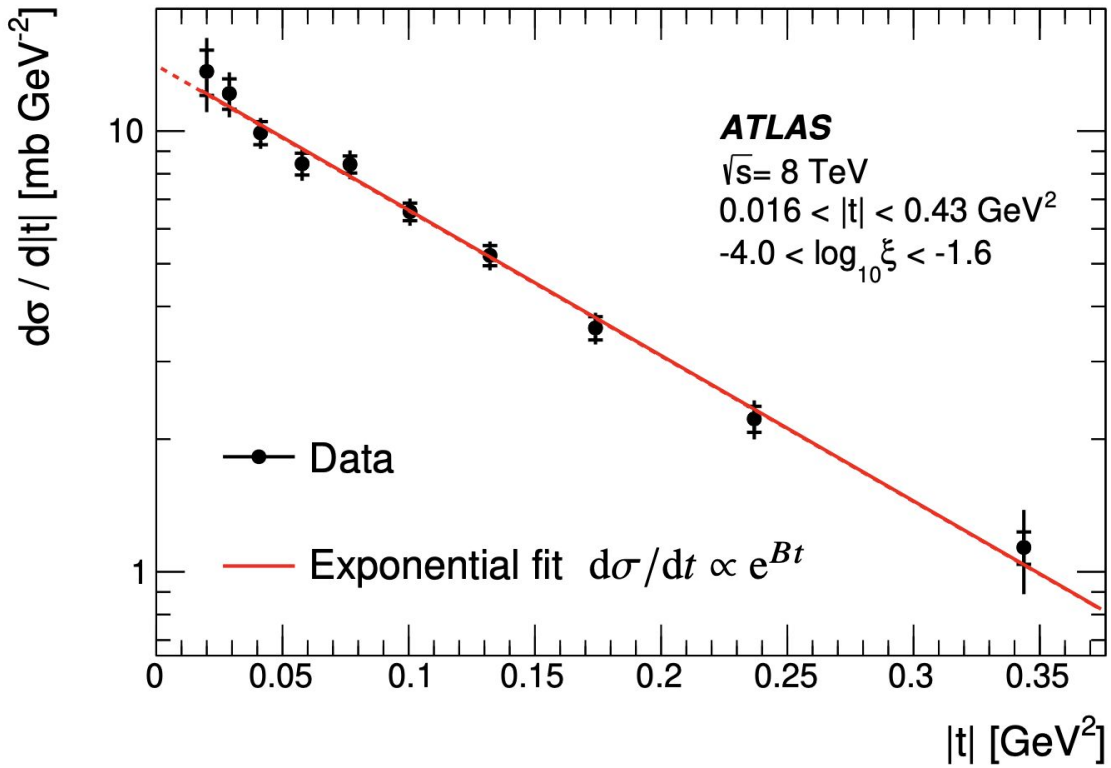

← Momentum transfer |t|

|t| measurements scarce at LHC
Compatible with exponential slope and both Pythia predictions

Generator predictions

From PHYS-PUB-2016-017

Pythia8 A2: B = 7.82 GeV^{-2}

Pythia8 A3 : B = 7.10 GeV^{-2}

Measurement

B = 7.65 ± 0.26 (stat.) ± 0.22 (syst.) GeV^{-2}

Systematics dominated by proton overlay backgrounds

JHEP 02 (2020) 042

ATLAS Forward Proton analysis

New instrument for standard high-luminosity LHC data-taking
First high-μ physics publication with AFP using 2017 dataset

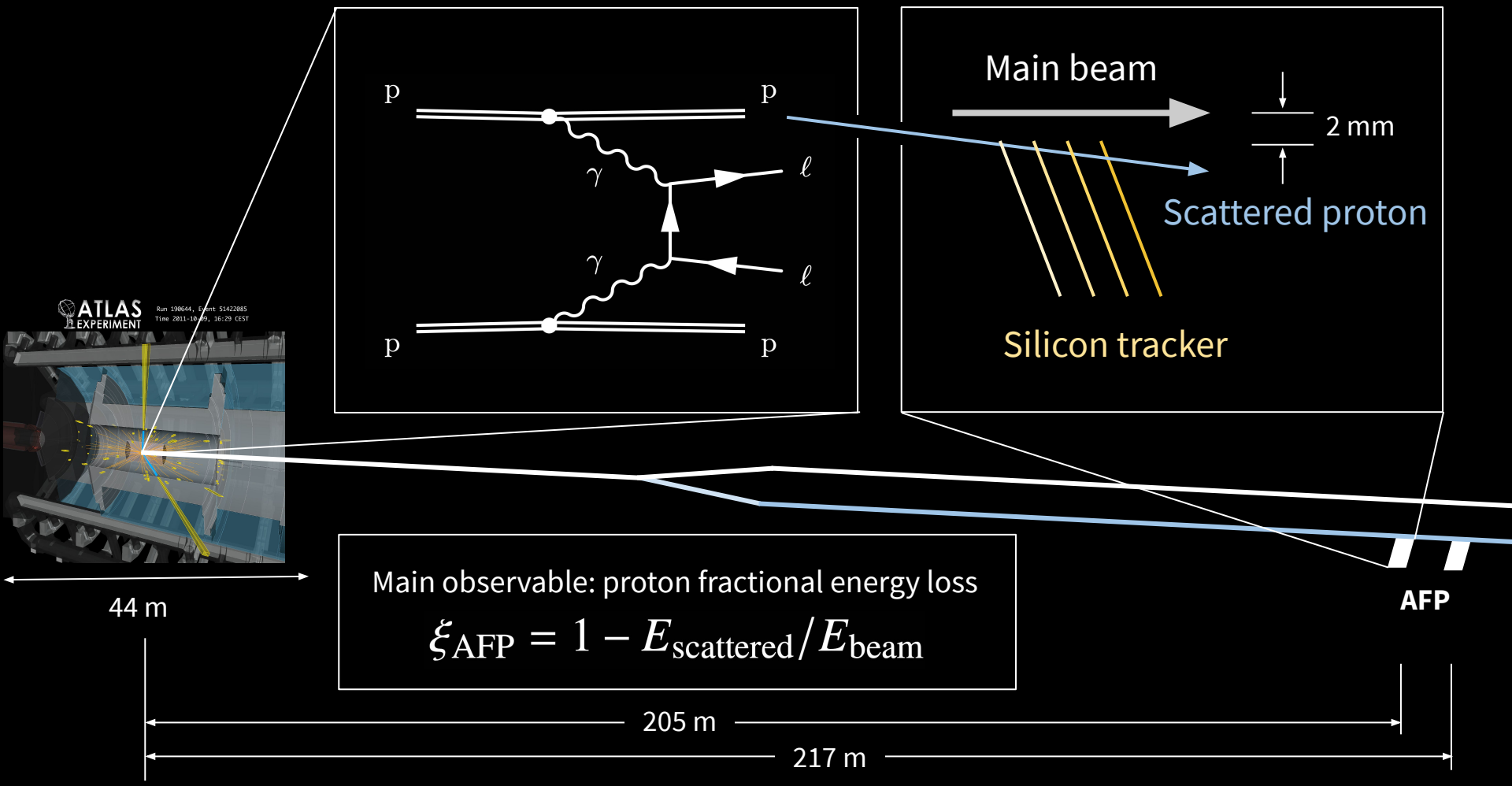

Main observable: proton fractional energy loss

$$\xi_{\mathrm{AFP}} = 1 - E_{\mathrm{scattered}}/E_{\mathrm{beam}}$$

Motivating $\gamma\gamma \to e^+e^-$: occurs in wide-ranging science

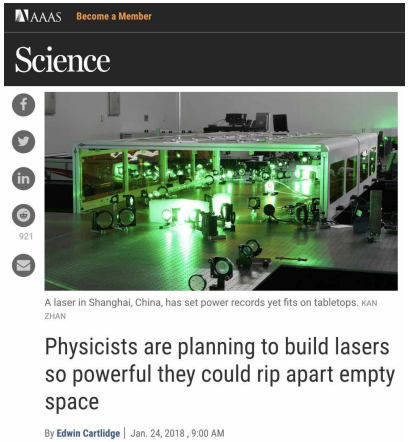

High intensity laser physics

Science Magazine News (2018), LUXE CDR [2102.02032]

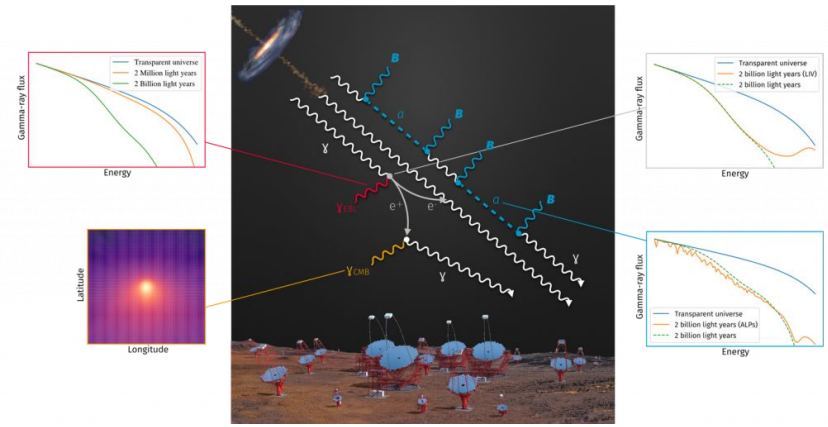

Cosmic gamma ray collisions

cta-observatory

Artist's impression of the magnetar in star cluster Westerlund 1. (Image: © ESO/L. Calçada)

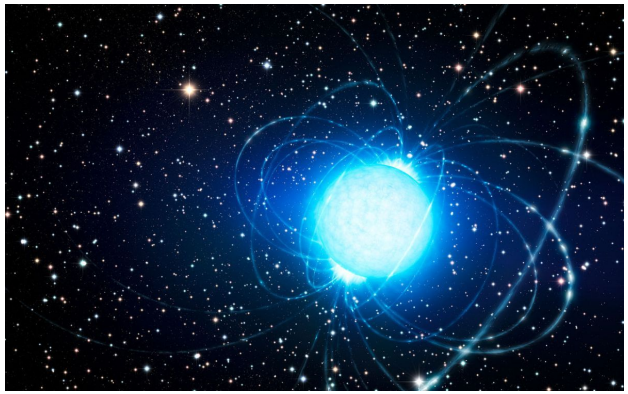

Magnetar neutron stars

Kaspi & Beloborodov [1703.00068]

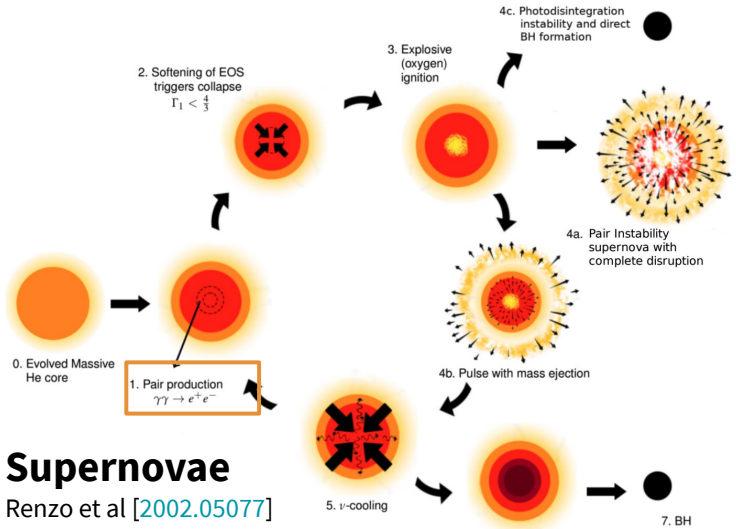

Supernovae

Renzo et al [2002.05077]

LHC can study photon fusion production at uncharted laboratory energies

Two measurements 210 m apart

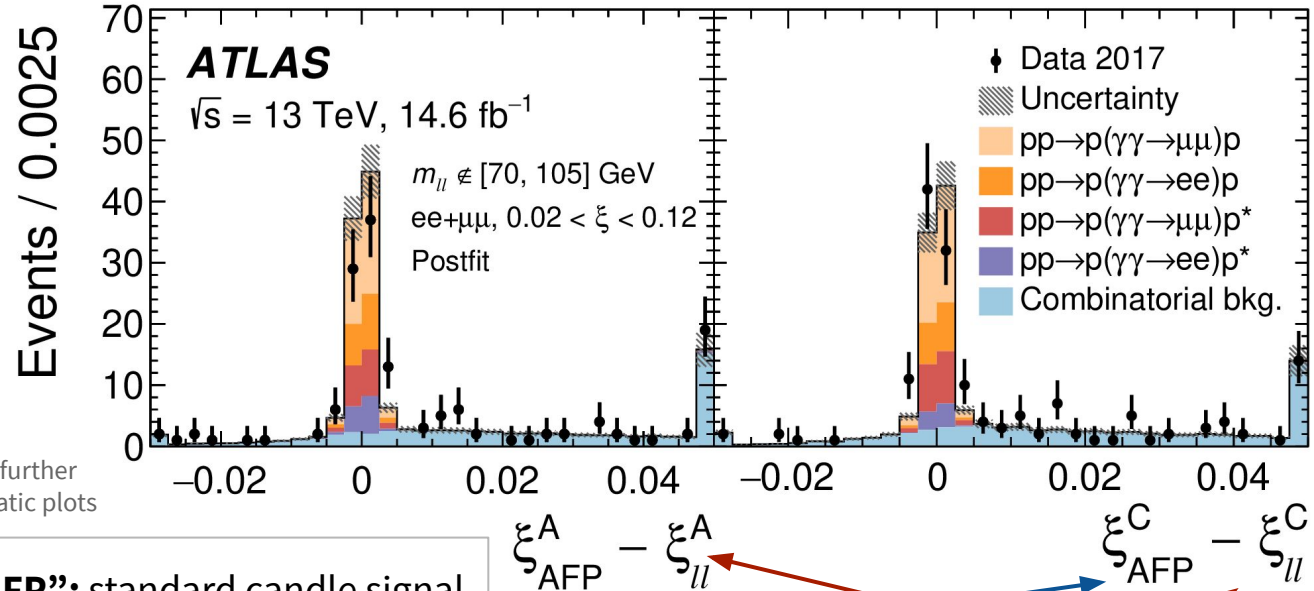

PRL 125 (2020) 261801
A = towards LHCb
C = towards ALICE

Selection details
$p_T(e/\mu) > 18/15$ GeV
$|z_{\ell\ell} - z_{trk}| > 0.5$ mm
$1 - |\Delta\phi_{\ell\ell}|/\pi < 0.01$
$p_T(\ell\ell) < 5$ GeV

See backup for further detailed kinematic plots

"J/ψ of AFP": standard candle signal

Direct: AFP spectrometer measures ξ_{AFP}

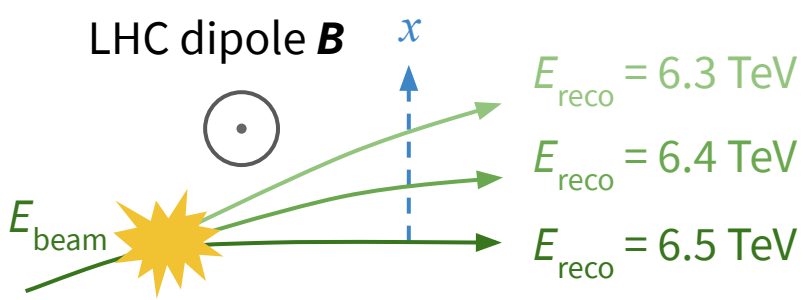

Indirect: central ATLAS measures $\xi_{\ell\ell}$

Measure lepton kinematics

$$\xi^{\pm}_{\ell\ell} = \frac{m_{\ell\ell}}{\sqrt{s}} e^{\pm y_{\ell\ell}} \qquad + = A, \; - = C$$

Infer proton kinematics*

*Formula analogous to parton Bjoken-x for PDFs

Signal vs background

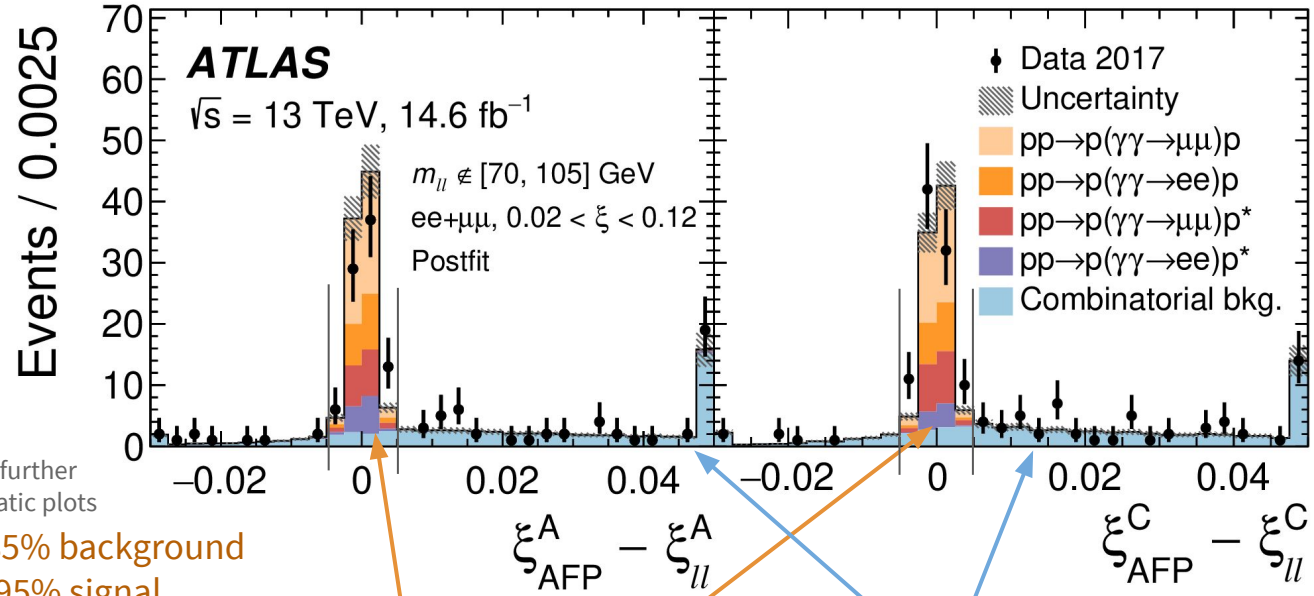

PRL 125 (2020) 261801
A = towards LHCb
C = towards ALICE

Selection details
$p_T(e/\mu) > 18/15$ GeV
$|z_{\ell\ell} - z_{trk}| > 0.5$ mm
$1 - |\Delta\phi_{\ell\ell}|/\pi < 0.01$
$p_T(\ell\ell) < 5$ GeV

See backup for further detailed kinematic plots

Cut rejects 85% background
And retains 95% signal

Signal: ξ_{AFP} & $\xi_{\ell\ell}$ kinematically correlated

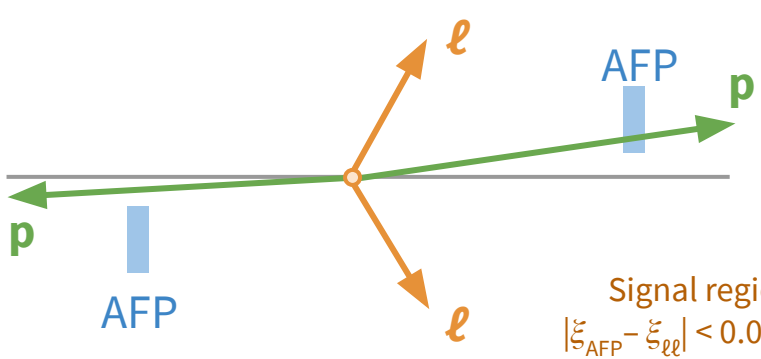

Bkg estimate: mix protons in data events

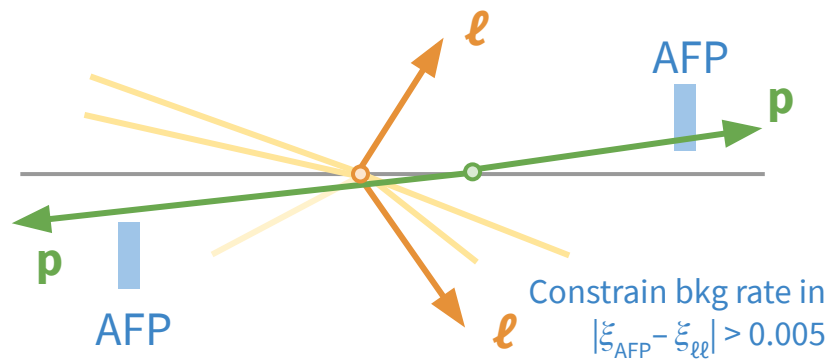

Dominated by Drell–Yan ($qq \to Z^{(*)}/\gamma^* \to \ell\ell$) + diffractive pileup

Kinematics of 180 (γγ → ℓℓ) + p candidates

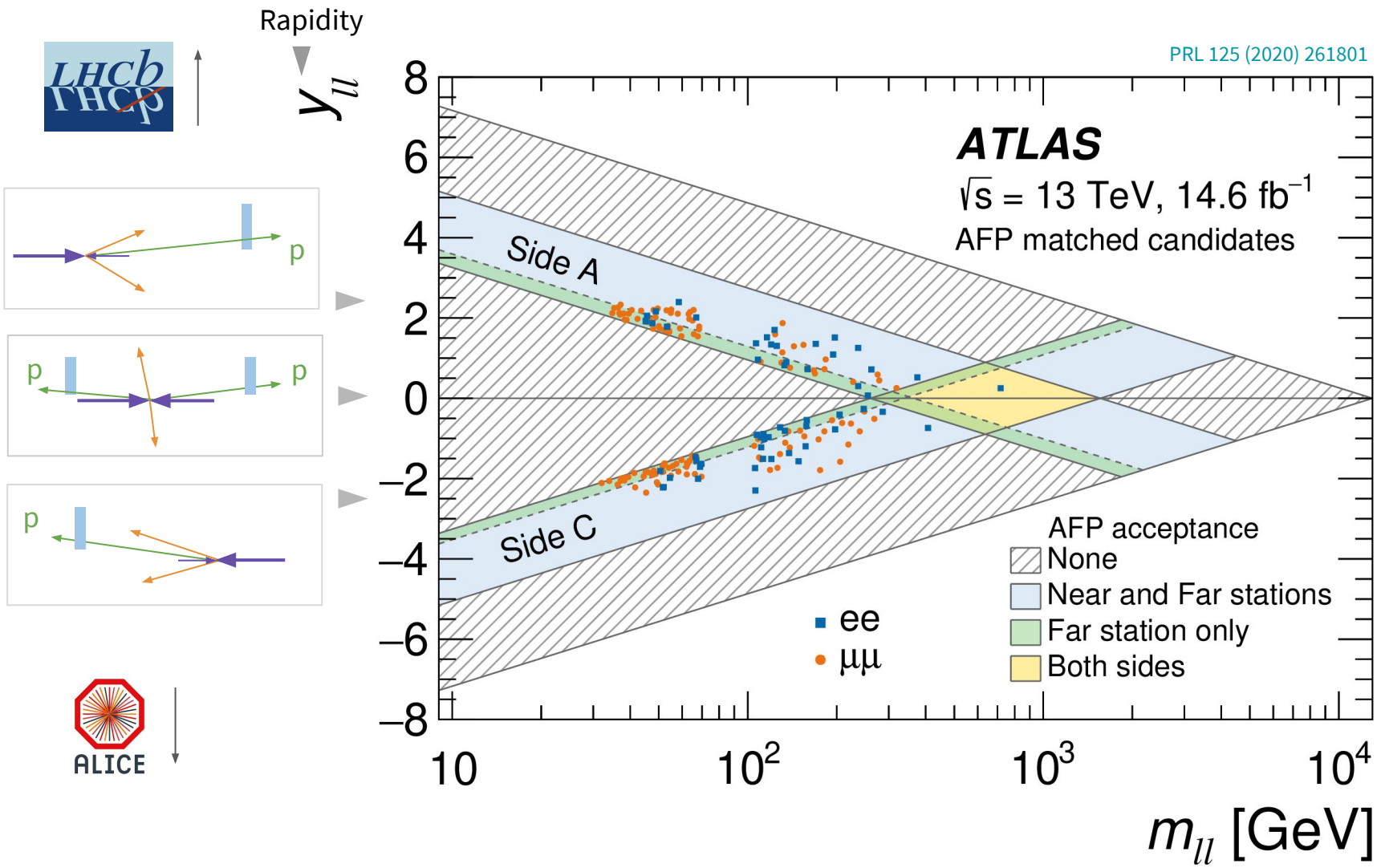

m_{ee} = 717 GeV event in both-side acceptance but side A fails $|\xi_{AFP} - \xi_{\ell\ell}| < 0.005$
So side A proton likely dissociated + pileup faked proton

Snapshot of results: observation & measurement

Data counts

	Observation	Measurement
ξ range	[0.02, 0.12]	[0.035, 0.08]
ee+p	57 (9.7σ)	19
μμ+p	123 (13σ)	23

PRL 125 (2020) 261801

First measurements of (γγ → ℓℓ) + p

$\sigma_{\text{HERWIG+LPAIR}} \times S_{\text{surv}}$	$\sigma^{\text{fid.}}_{ee+p}$ (fb)	$\sigma^{\text{fid.}}_{\mu\mu+p}$ (fb)
$S_{\text{surv}} = 1$	15.5 ± 1.2	13.5 ± 1.1
S_{surv} using Refs. [33, 34]	10.9 ± 0.8	9.4 ± 0.7
SUPERCHIC 4 [97]	12.2 ± 0.9	10.4 ± 0.7
Measurement	11.0 ± 2.9	7.2 ± 1.8

$$\sigma_{\text{fid.}} = (N_{\text{obs}} - N_{\text{bkg}})/(\mathcal{L} \cdot C_{\text{cent}} \cdot C_{\text{AFP}})$$

PRL 125 (2020) 261801

Performance: AFP detector efficiencies & stability

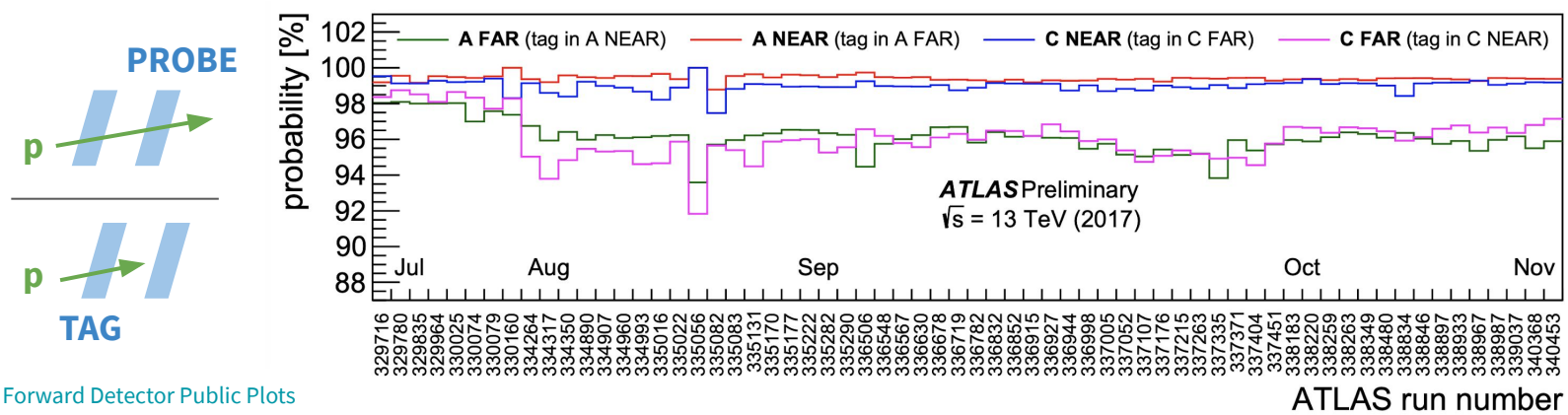

Forward Detector Public Plots

S_{surv} = proton soft survival probability from non-perturbative QCD dynamics

[33, 34] = Harland-Lang et al EPJC 76 (2016) 255, Dyndal & Schoffel PLB 741 (2015) 66;
[97] = Harland-Lang et al EPJC 80 (2020) 925

Importance & outlook

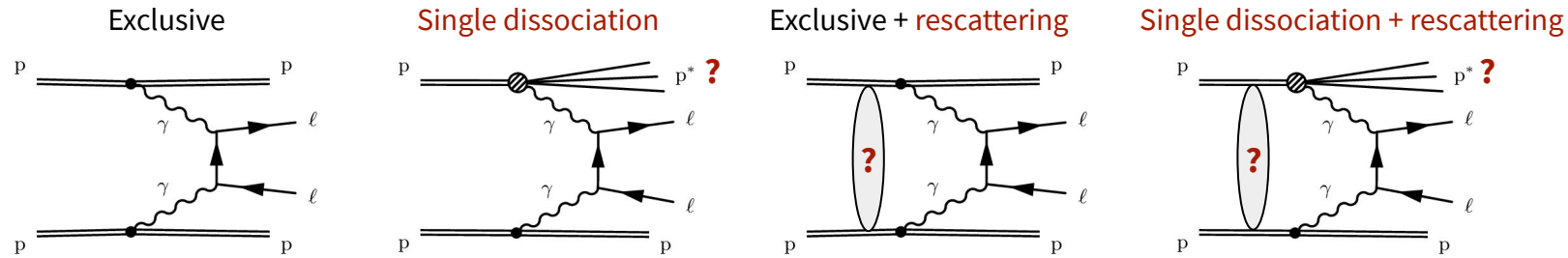

Soft QCD dissociation and rescattering important for precision but challenging to experimentally probe and reliably predict

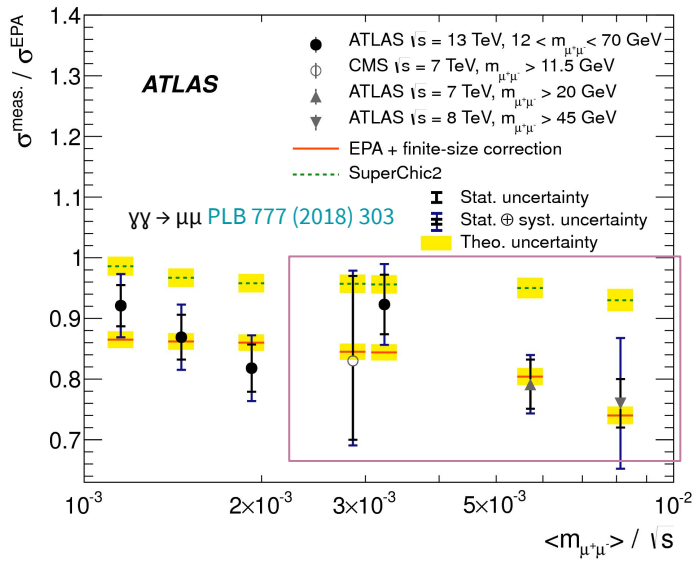

SD subtracted via central kinematics (non-AFP)
Likely rescattering effects for excl and/or SD

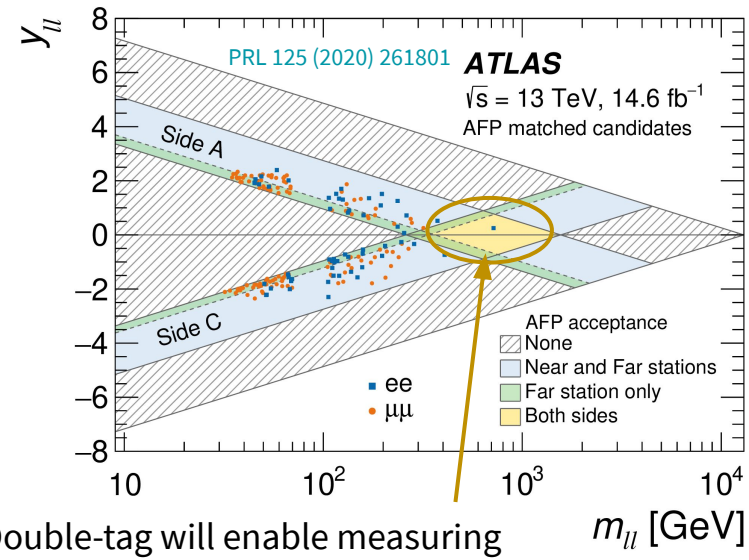

Double-tag will enable measuring
pp → p + (γγ→ℓℓ) + p (exactly 2) independent from
pp → p + (γγ→ℓℓ) (exactly 1) in same phase space

Previous: data also ~10% below Superchic2 MC

Future: use AFP to directly separate excl vs SD

Can also indirectly probe double dissociation by measuring e.g. pT(ℓℓ)

SUMMARY

Proton tagging expands our repertoire to probe the microcosm

pp → p+X: important low-μ single-diffraction measurements using ALFA detector
pp → p(γγ → ℓℓ)p(*): introduced proton tagging to high-μ measurements with AFP

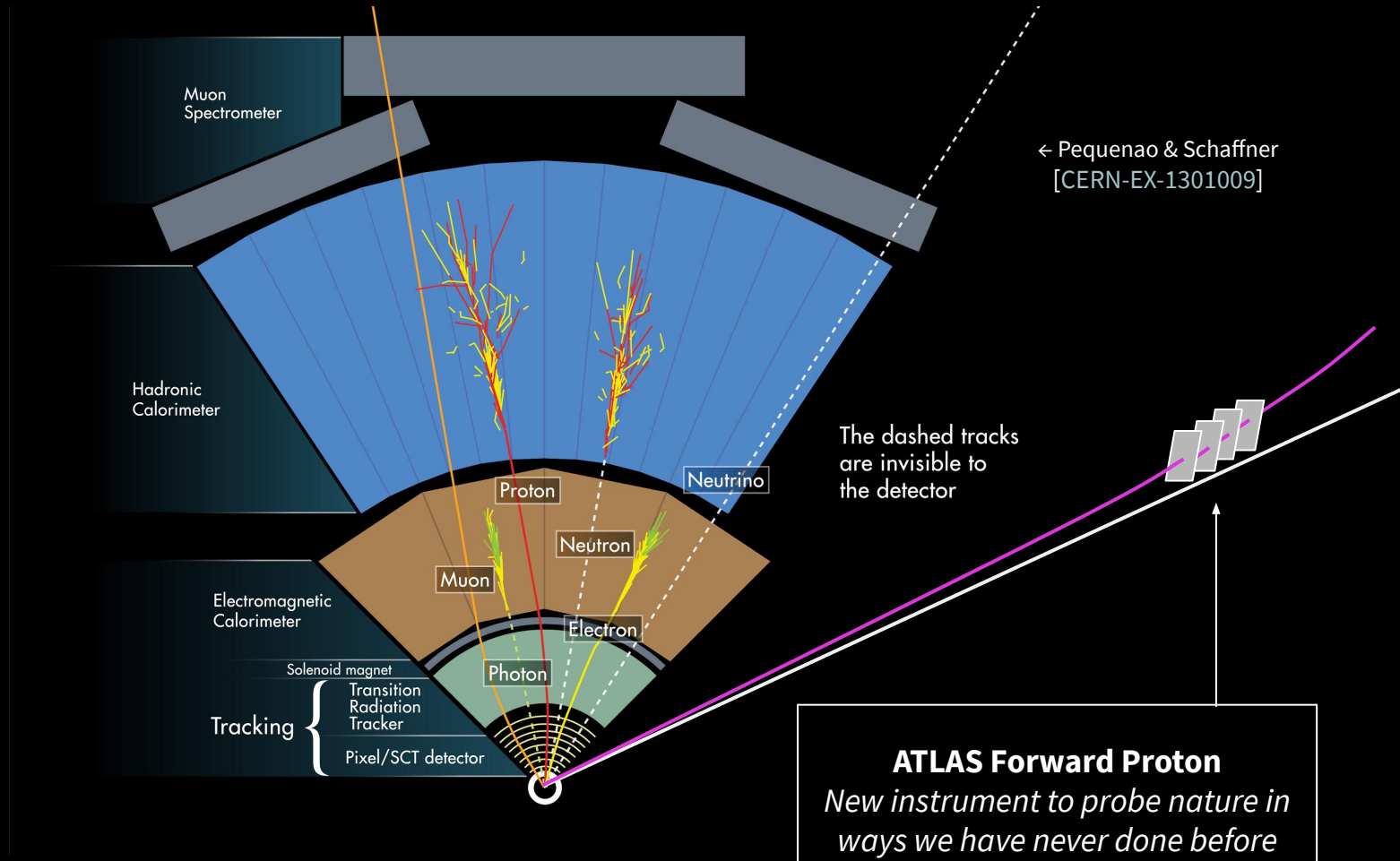

ATLAS Forward Proton
New instrument to probe nature in ways we have never done before

EXTRAS

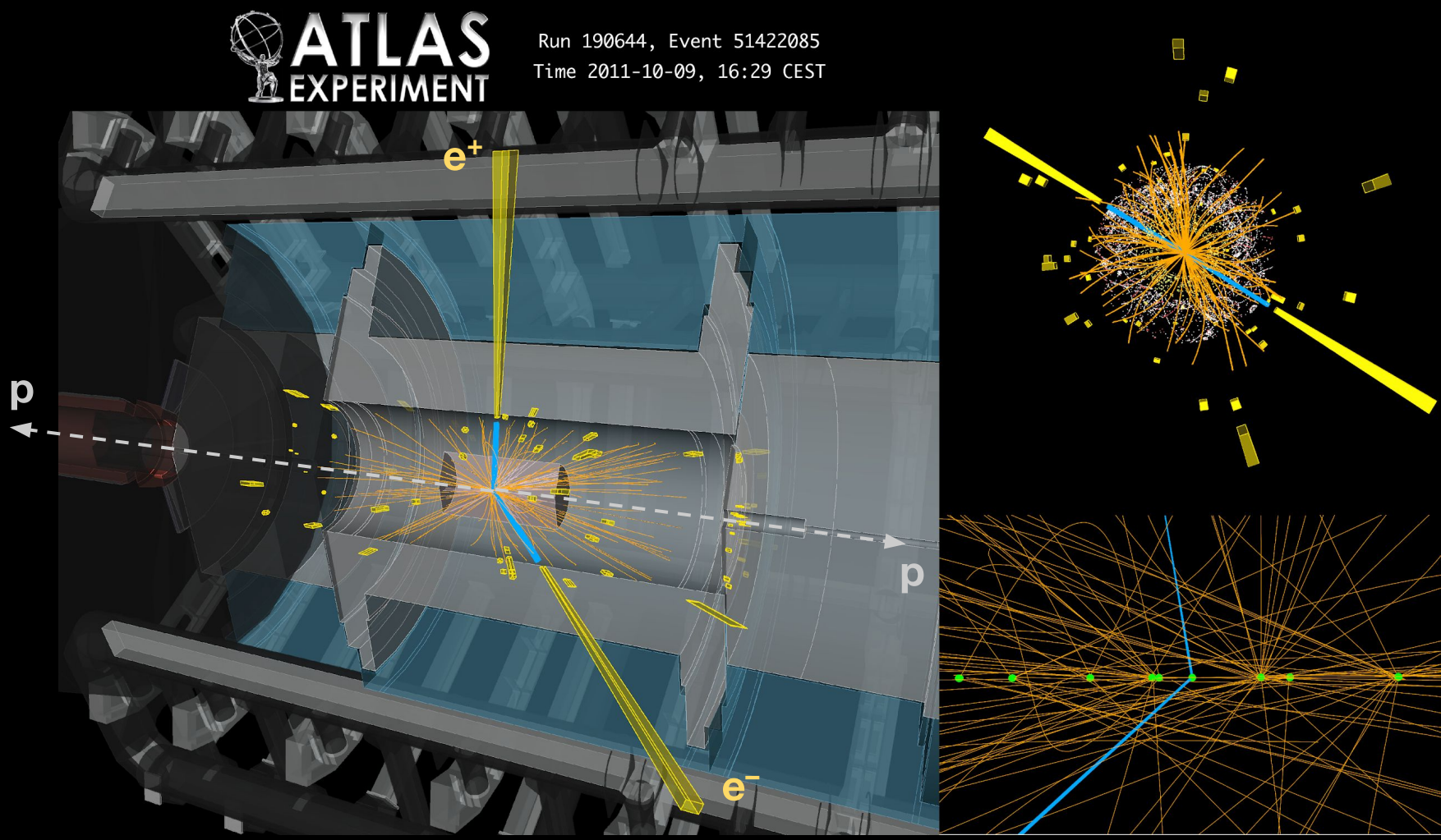

γγ → ee @ 7 TeV event display [1506.07098]
See also γγ → μμ @ 13 TeV [1708.04053]

$$pp \to p + \underbrace{(\gamma\gamma \to ee)} + p$$

Without AFP can only see this

With AFP: directly observe intact protons

First high-μ physics publication with AFP

PHYSICAL REVIEW LETTERS **125**, 261801 (2020)

[PRL 125 (2020) 261801]

Observation and Measurement of Forward Proton Scattering in Association with Lepton Pairs Produced via the Photon Fusion Mechanism at ATLAS

G. Aad *et al.*[*]
(ATLAS Collaboration)

(Received 2 October 2020; revised 30 October 2020; accepted 23 November 2020; published 23 December 2020)

Physics Briefing

[ATLAS Physics Briefing]

Tags: Physics Results, ICHEP2020, ICHEP, forward detectors

Looking forward: ATLAS measures proton scattering when light turns into matter

By ATLAS Collaboration, 30th July 2020

Today, at the International Conference for High Energy Physics (ICHEP 2020), the ATLAS Collaboration announced first results using the ATLAS Forward Proton (AFP) spectrometer (Figure 1). With this instrument, physicists directly observed and measured the long sought-after prediction of proton scattering when particles of light turn into matter.

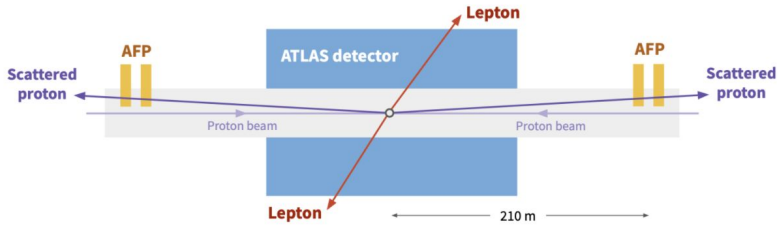

Figure 1: Schematic diagram of ATLAS Forward Proton (AFP) spectrometer relative to the main ATLAS detector (not to scale). After the incident proton beams intersect, the leptons are detected by the main ATLAS detector and the scattered proton is detected by AFP. (Image: ATLAS Collaboration/CERN)

[CERN Courier Sep/Oct 2020 Issue]

CERNCOURIER.COM

ENERGY FRONTIERS

Reports from the Large Hadron Collider experiments

ATLAS

The LHC as a photon collider

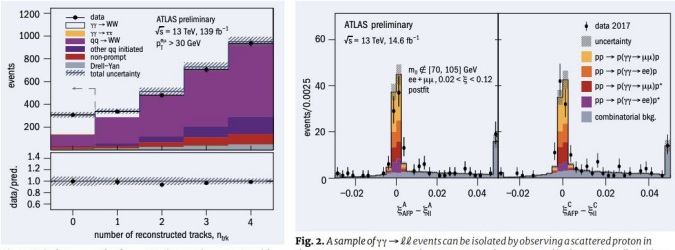

Fig. 1. *To isolate a sample of $\gamma\gamma \to WW$ interactions, events with no additional reconstructed charged-particle tracks in the vicinity of the electron–muon pair ($n_{trk} = 0$) are selected.*

Fig. 2. *A sample of $\gamma\gamma \to \ell\ell$ events can be isolated by observing a scattered proton in the AFP spectrometer. Here, the proton energy loss measured in the AFP installed either side (A and C) of the collision point (ξ_{AFP}, dimensionless) is shown to agree with that predicted from measurements of the lepton pair in the main detector ($\xi_{\ell\ell}$).*

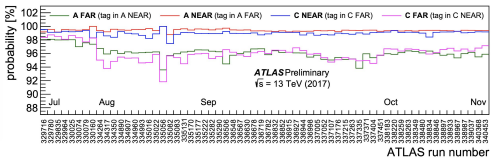

Data quality & efficiencies

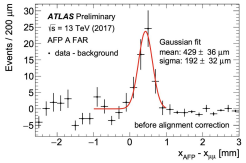

In situ calibration

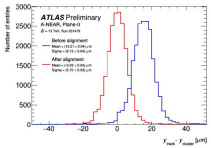

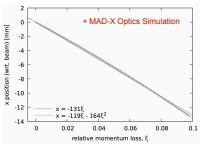

Source of systematic uncertainty	Impact
Forward detector	
Global alignment	6%
Beam optics	5%
Resolution and kinematic matching	3–5%
Track reconstruction efficiency	3%
Alignment rotation	1%
Clustering and track-finding procedure	< 1%

Alignment Simulation Systematics

Pioneering detector performance work

AFP from design to data

TDR

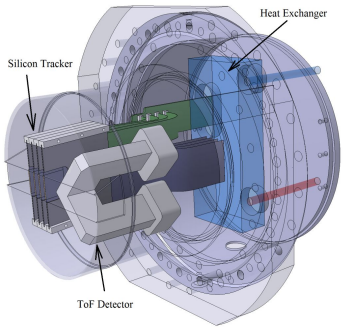

ATLAS Forward Proton
Phase-I Upgrade

Technical Design Report

ATL-TDR-024 (2015)

Technical simulation
For LHC Run 2 installation

Prototype

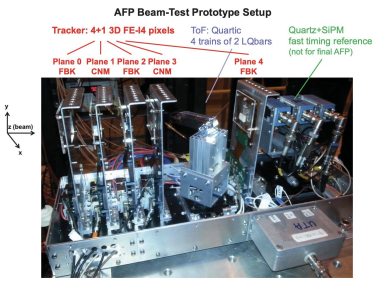

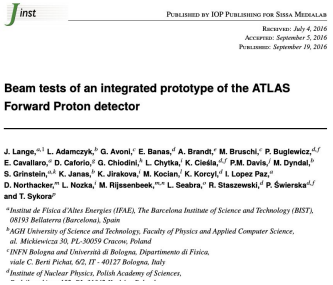
Jinst
Published by IOP Publishing for Sissa Medialab
Received: July 4, 2016
Accepted: September 5, 2016
Published: September 19, 2016

Beam tests of an integrated prototype of the ATLAS Forward Proton detector

J. Lange,[a,1] L. Adamczyk,[b] G. Avoni,[c] E. Banas,[d] A. Brandt,[e] M. Bruschi,[c] P. Buglewicz,[d,f] E. Cavallaro,[g] D. Caforio,[g] G. Chiodini,[h] L. Chytka,[i] K. Cieśla,[d,f] P.M. Davis,[i] M. Dyndal,[b] S. Grinstein,[a,j] K. Janas,[d] K. Jirakova,[i] M. Kocian,[i] K. Korcyl,[d] I. Lopez Paz,[g] D. Northacker,[m] L. Nozka,[i] M. Rijssenbeek,[m,n] L. Seabra,[o] R. Staszewski,[d] P. Świerska[d,f] and T. Sykora[p]

[a]Institut de Física d'Altes Energies (IFAE), The Barcelona Institute of Science and Technology (BIST), 08193 Bellaterra (Barcelona), Spain
[b]AGH University of Science and Technology, Faculty of Physics and Applied Computer Science, al. Mickiewicza 30, PL-30059 Cracow, Poland
[c]INFN Bologna and Università di Bologna, Dipartimento di Fisica, viale C. Berti Pichat, 6/2, IT - 40127 Bologna, Italy
[d]Institute of Nuclear Physics, Polish Academy of Sciences,

JINST 11 (2016) P09005

Beam tests
Integrated prototype

Single arm low-μ

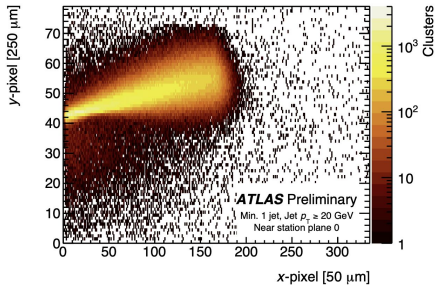

ATLAS NOTE
ATL-PHYS-PUB-2017-012
29th June 2017

Proton tagging with the one arm AFP detector

The ATLAS Collaboration

ATL-PHYS-PUB-2017-012

Data 2016
Diffractive jets performance

Double arm high-μ

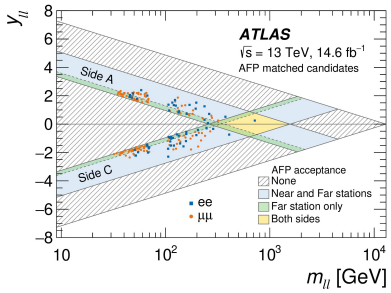

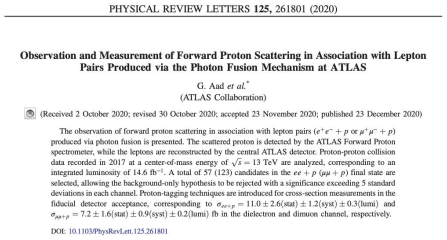
PHYSICAL REVIEW LETTERS 125, 261801 (2020)

Observation and Measurement of Forward Proton Scattering in Association with Lepton Pairs Produced via the Photon Fusion Mechanism at ATLAS

G. Aad et al.*
(ATLAS Collaboration)

(Received 2 October 2020; revised 30 October 2020; accepted 23 November 2020; published 23 December 2020)

The observation of forward proton scattering in association with lepton pairs ($e^+e^- + p$ or $\mu^+\mu^- + p$) produced via photon fusion is presented. The scattered proton is detected by the ATLAS Forward Proton spectrometer, while the leptons are reconstructed by the central ATLAS detector. Proton-proton collision data recorded in 2017 at a center-of-mass energy of $\sqrt{s} = 13$ TeV are analyzed, corresponding to an integrated luminosity of 14.6 fb^{-1}. A total of 57 (123) candidates in the $ee + p$ ($\mu\mu + p$) final state are selected, allowing the background-only hypothesis to be rejected with a significance exceeding 5 standard deviations in each channel. Proton-tagging techniques are introduced for cross-section measurements in the fiducial detector acceptance, corresponding to $\sigma_{ee+p} = 11.0 \pm 2.6(\text{stat}) \pm 1.2(\text{syst}) \pm 0.3(\text{lumi})$ and $\sigma_{\mu\mu+p} = 7.2 \pm 1.6(\text{stat}) \pm 0.9(\text{syst}) \pm 0.2(\text{lumi})$ fb in the dielectron and dimuon channel, respectively.

DOI: 10.1103/PhysRevLett.125.261801

NEW!

PRL 125 (2020) 261801

Data 2017
(γγ → ℓℓ)+p measurement

Today: highlight in situ AFP detector performance & innovations with recent LHC data

Towards vibrant AFP science programme

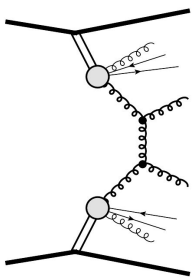

Diffractive jets
ATLAS PHYS-PUB-2017-012
CMS+TOTEM 2002.12146

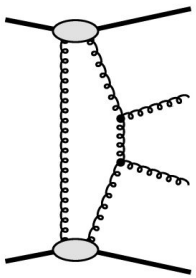

Exclusive jets
Khoze et al hep-ph/0605113
Trzebinski et al 1503.00699

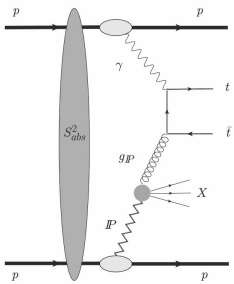

Top quarks
Goncalves et al 2007.04565
Howarth 2008.04249

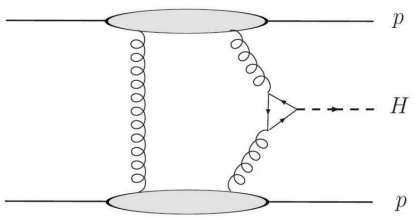

Higgs boson
Cox et al 0709.3035
Heinemeyer et al 0708.3052

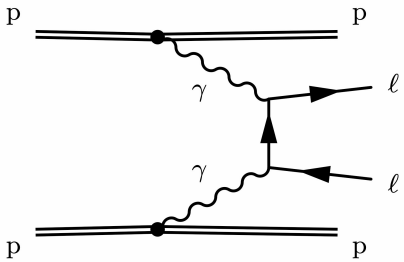

Leptons
CMS+TOTEM 1803.04496
ATLAS 2009.14537

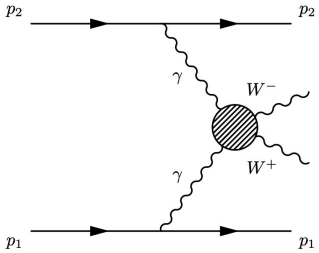

W bosons
Tizchang & Etesami 2004.12203
Baldenegro et al 2009.08331

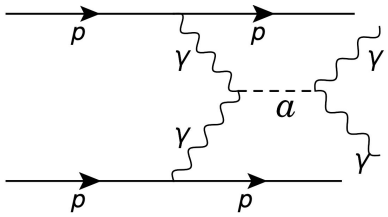

Axion-like particles
Fichet et al 1312.5153
Baldenegro et al 1803.10835

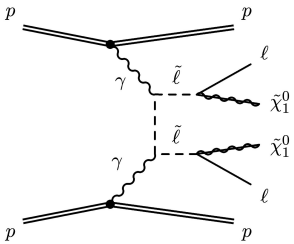

SUSY dark matter
Beresford & JL 1811.06465
Harland-Lang et al 1812.04886

AFP Run 2 data: important probes of QCD, electroweak & BSM physics ongoing

Significant Run 3 gains 150 fb^{-1}/14.6 fb^{-1} ⇒ up to 10x lumi + 20 ps time-of-flight

LHC: a laboratory for studying photon collisions

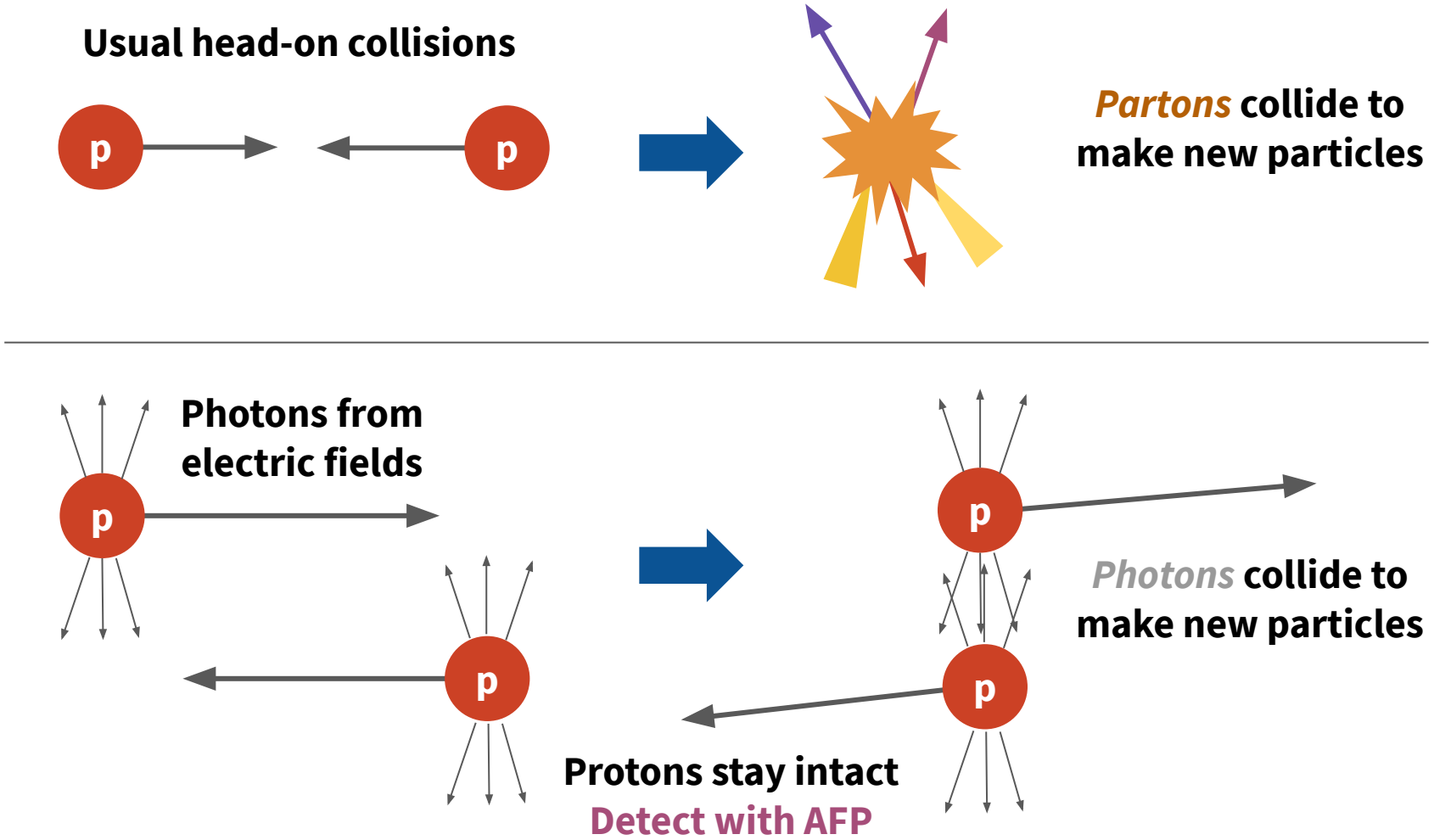

Fermi (1925) [hep-th/0205086], Breit & Wheeler (1934), Weizsäcker (1934), Williams (1934), Heisenberg & Euler (1936), Schwinger (1952) Brodsky, Kinoshita, Terazaw (1971), Budnev, Ginzburg, Meledin, Serbo (1975), Khoze, Martin, Ryskin [hep-ph/0201301] Bruce et al [1812.07688], Klein & Steinberg [2005.01872]

Colliding γγ spectrum

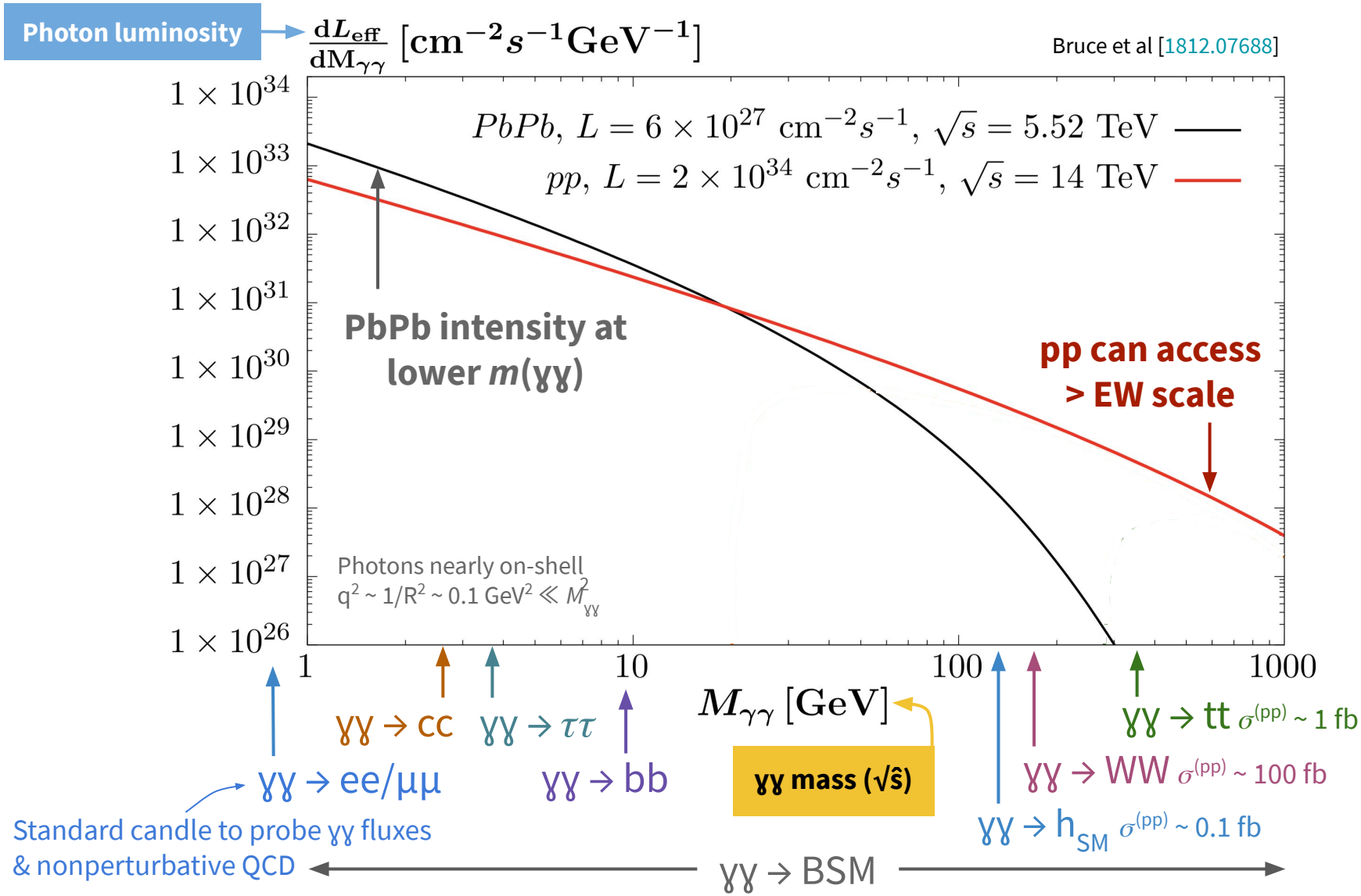

How AFP qualitatively changes the game

LEPTON COLLIDER

All initial & visible final state 4-vectors measurable

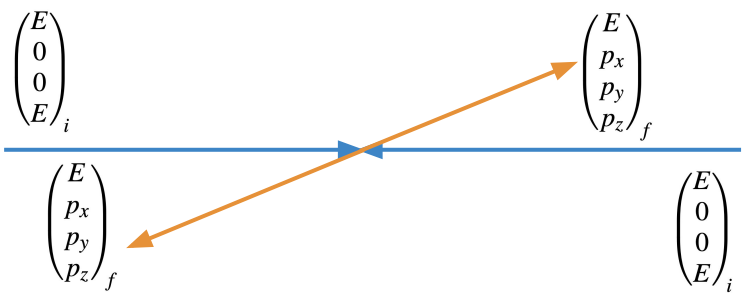

HADRON COLLIDER (NO AFP)

p^{z}_{initial} immeasurable

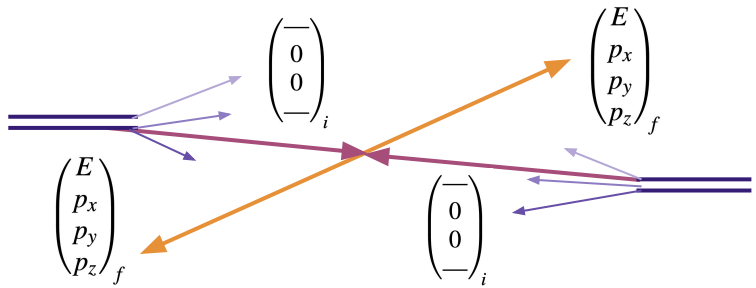

HADRON COLLIDER (+ AFP)

⇒ Full p_{initial} measurable

New event kinematic information!

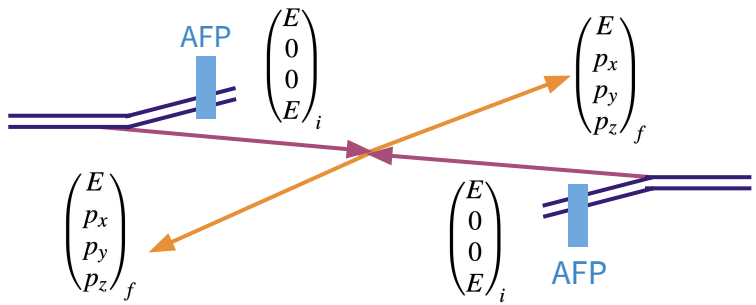

Colliding photon energy measurable in data

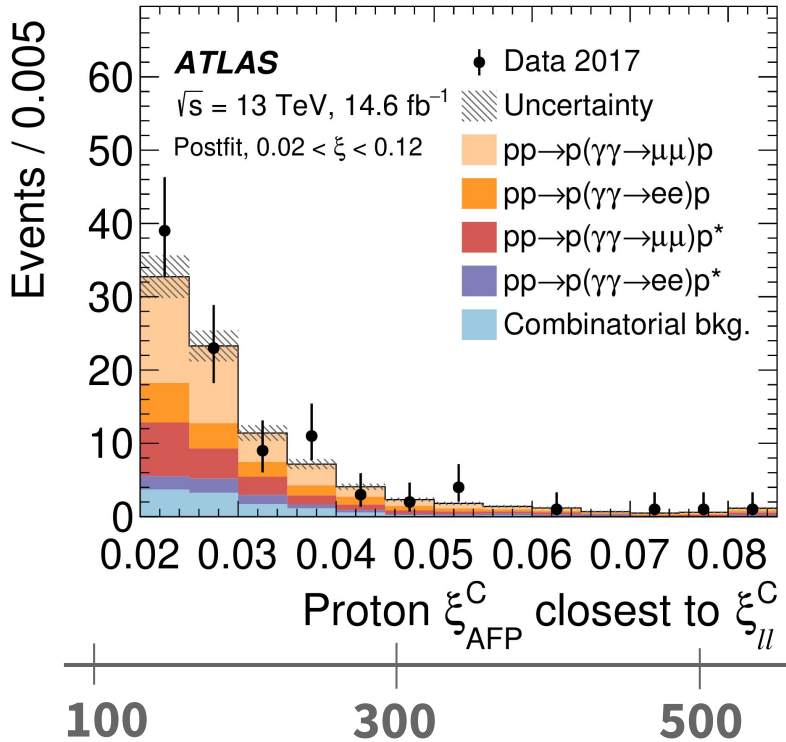

ATLAS [2009.14537]

Details for interested experts

2ℓ triggers, $p_T(e/\mu) > 18/15$ GeV, $|z_{\ell\ell} - z_{trk}| > 0.5$ mm, $m_{\ell\ell} \notin [70, 105]$ GeV, $|\Delta\phi_{\ell\ell}|/\pi > 0.99$, $p_T(\ell\ell) < 5$ GeV

p* = proton dissociates after EM excitation and undetected

FUTURE GOAL

Enables p_{miss} 4-vector & dark matter mass

Otherwise impossible without AFP

$$p_{\text{miss}} = \sum_{\text{initial}} p_i - \sum_{\text{final}} p_f^{\text{visible}} \quad \Rightarrow \quad m^2_{\text{miss}} = p^2_{\text{miss}}$$

$$E_\gamma = \xi E_{\text{beam}} \text{ [GeV]}$$

HADRON COLLIDER (+ AFP)

⇒ Full $p_{initial}$ measurable

New event kinematic information!

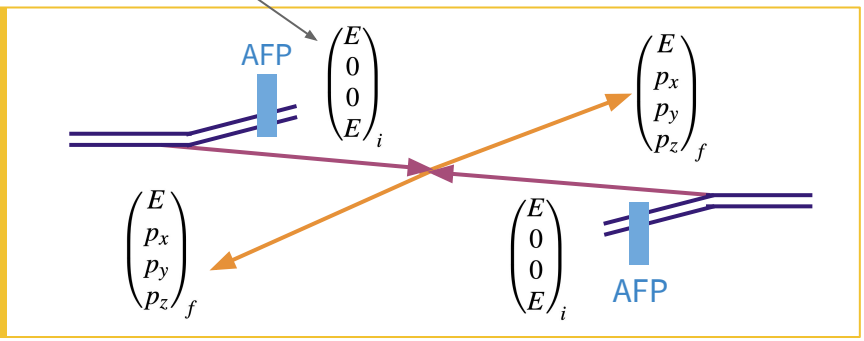

AFP DETECTOR

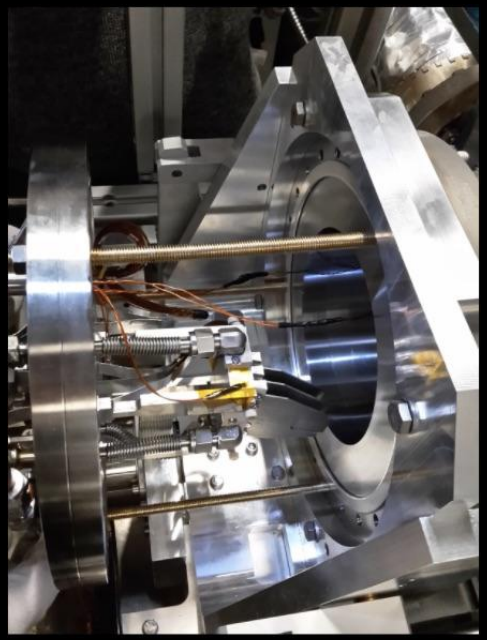

ROMAN POT

Insertion into beam pipe
40mm → 2mm when stable

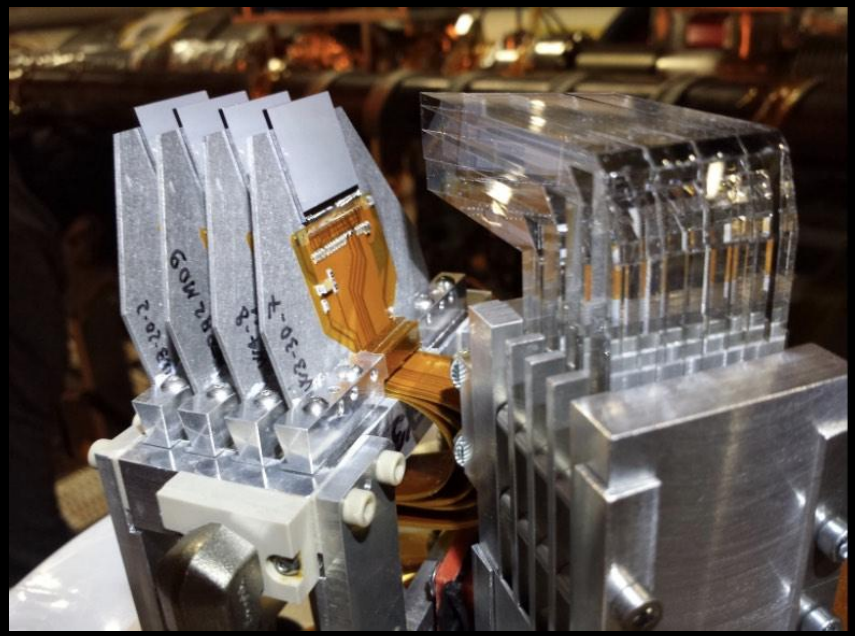

TRACKER & TIME-OF-FLIGHT

3D silicon pixels σ_x ~ 10 µm
Quartz Cerenkov bars σ_t ~ 30 ps*

INSTALLATION

One side 2016*
Both sides 2017

Adamczyk et al [AFP TDR]
* Not used in this talk

Colliders are laboratory for extreme QED

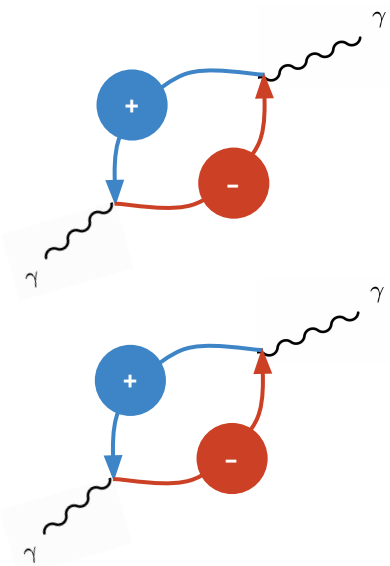

$\Delta E \Delta t \sim \hbar/2$
⇒ virtual loops polarise vacuum

Quantum vacuum

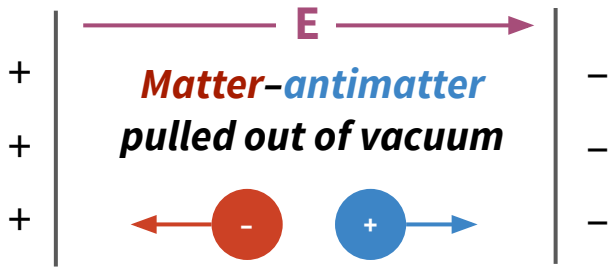

Matter–antimatter pulled out of vacuum

Work done on charges by E field in $\lambda_{Compton}$*

Pair production threshold

$$eE_{\text{crit}}\left(2\frac{\hbar}{m_e c}\right) \sim 2m_e c^2$$

$$\Rightarrow E_{\text{crit}} = \frac{m_e^2 c^3}{e\hbar} \sim 10^{18}\ \text{V m}^{-1}$$

$$B_{\text{crit}} = \frac{m_e^2 c^2}{e\hbar} \sim 10^{9}\ \text{T}$$

Schwinger limit

B ~ 10^{15} T @ RHIC

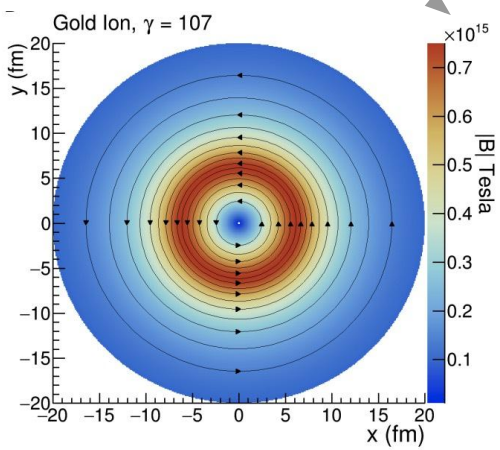

STAR [1910.12400]

Even stronger fields at LHC

Extreme QED in the lab

*Semiclassical intuition: full field-theoretic calculation requires non-perturbative QED [Schwinger 1952]

Detailed schematic

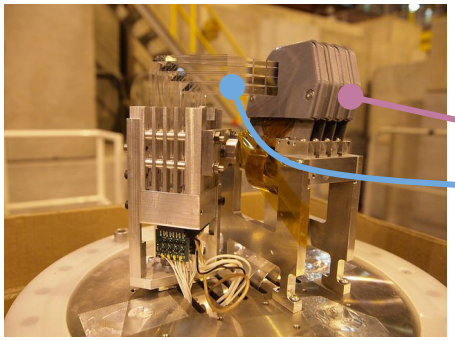

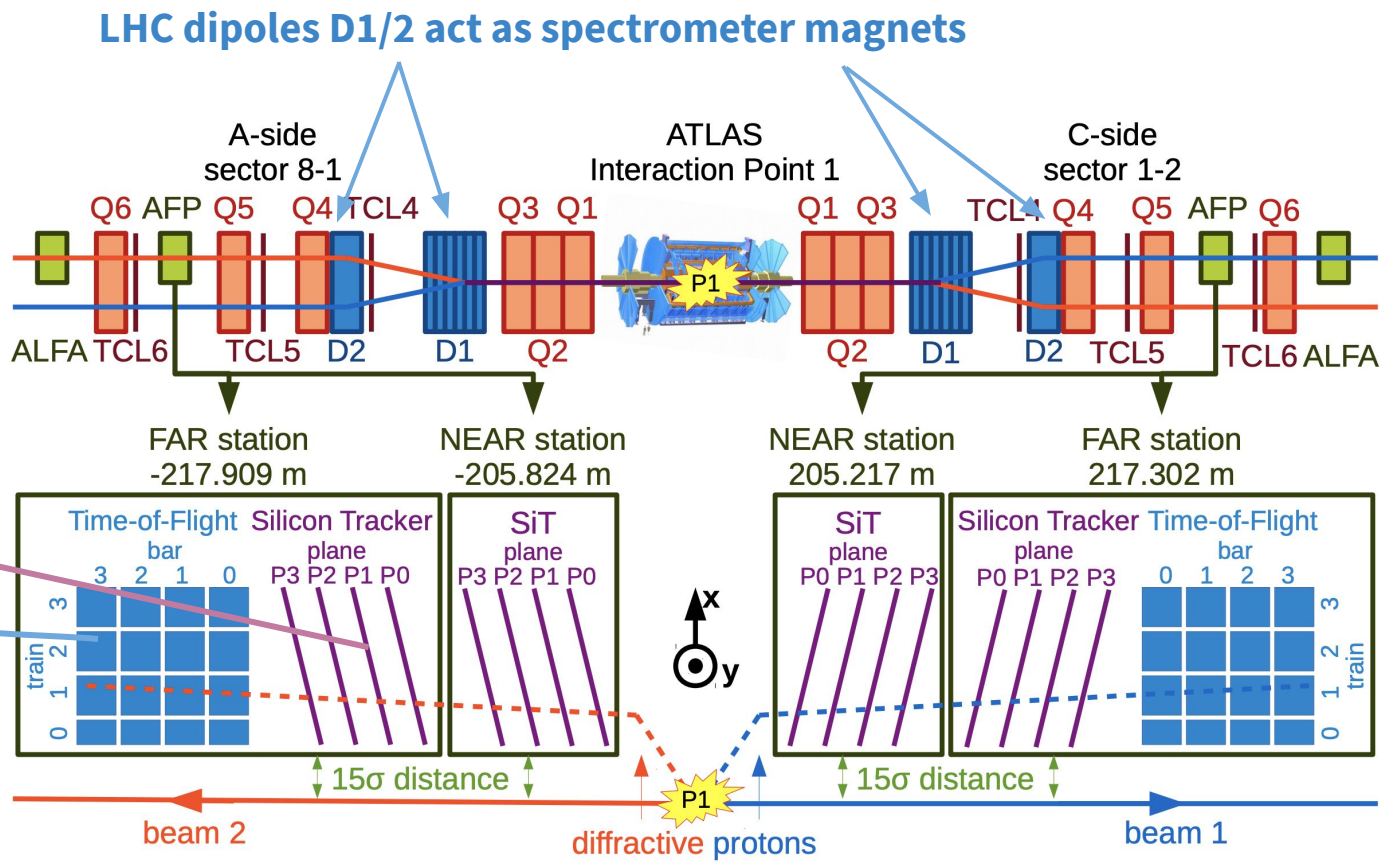

Towards Point 8 (LHCb)

Towards Point 2 (ALICE)

Global alignment scale calibration: importance & idea

Global absolute offset

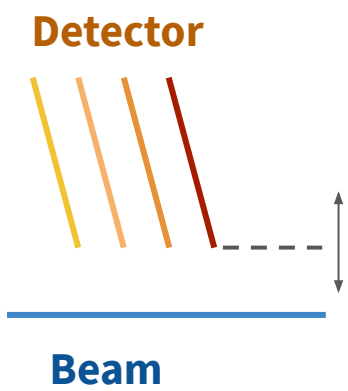

MAD-X beam propagation simulation

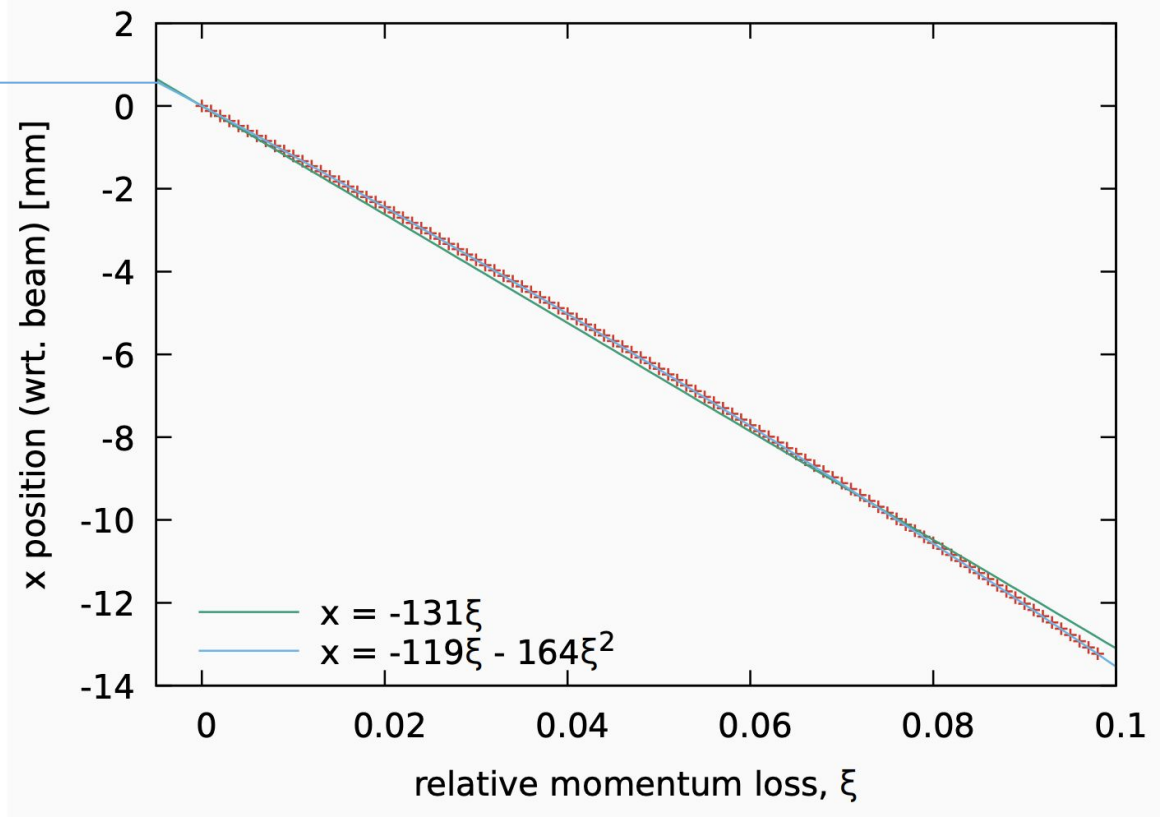

Spectrometer:
Instrument turning ***spatial measurements*** into ***energy measurements***

Directly impacts reconstructed fractional proton energy loss ξ

Beam based alignment: in practice

Sharp signal spike in BLM when beam is probed

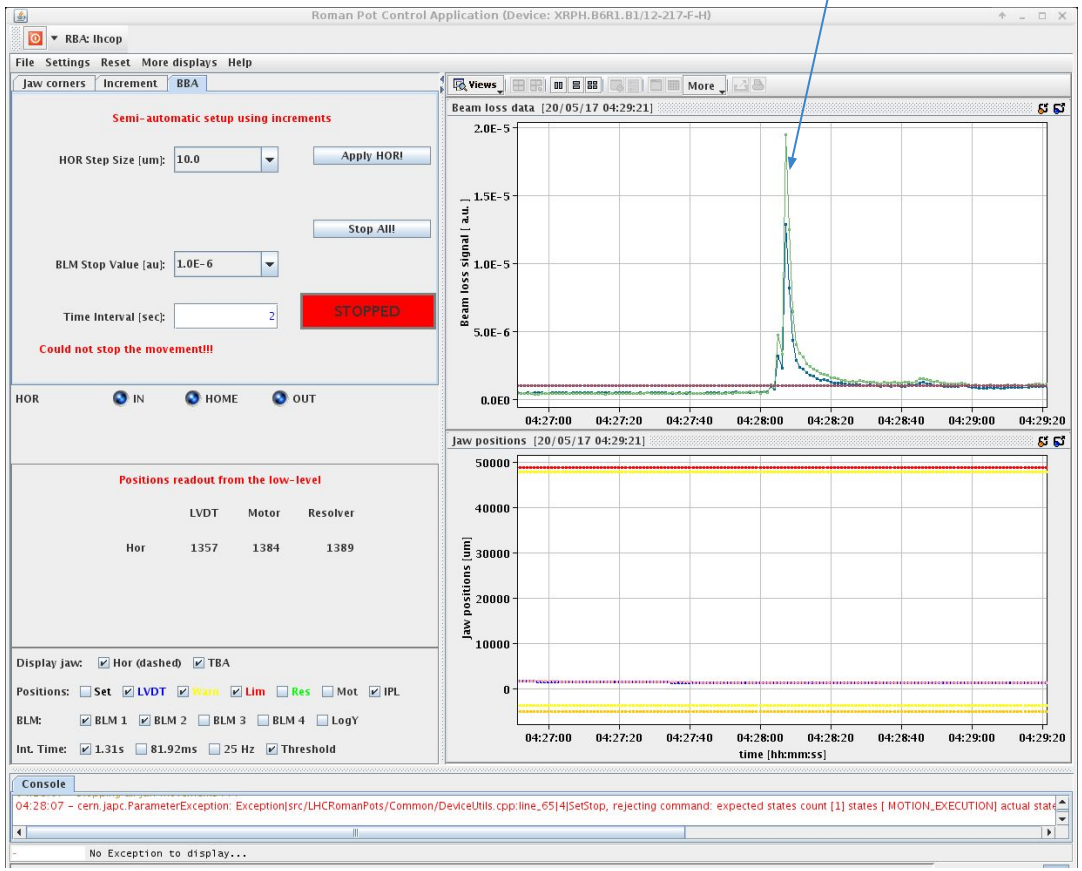

LHC operations: 20 May 2017

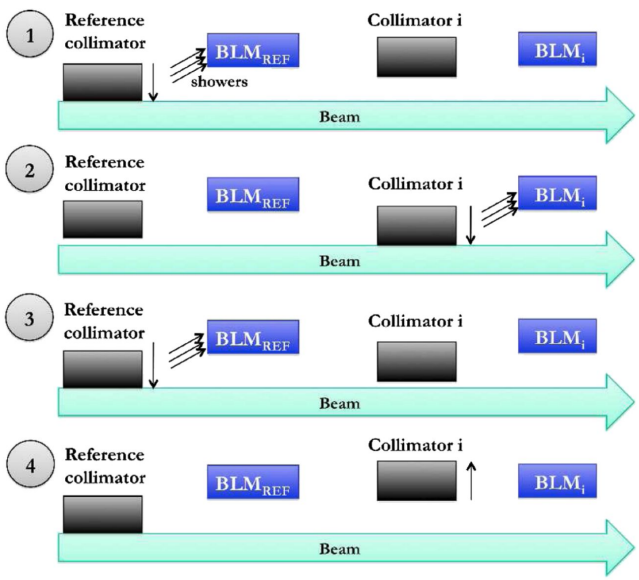

FIG. 4. The four-stage beam-based alignment procedure for collimator *i*. The reference collimator is aligned to form a reference cut in the beam halo (1). Collimator *i* is aligned (2), followed by a realignment of the reference collimator (3). Finally, collimator *i* is opened to its position in the hierarchy (4).

In situ dimuon calibration: fit & shift residuals

Use (γγ → μμ)+p signal as standard candle: "The J/ψ of AFP"

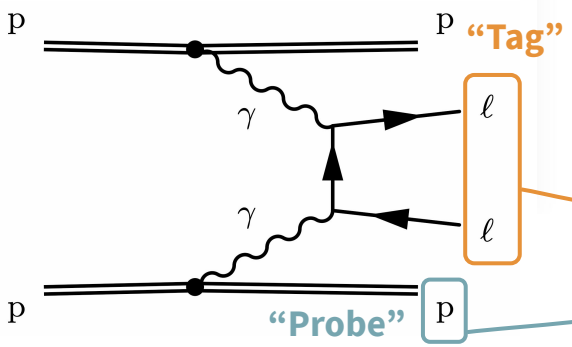

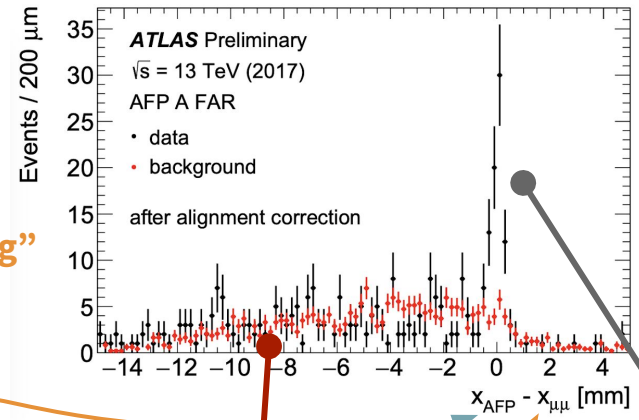

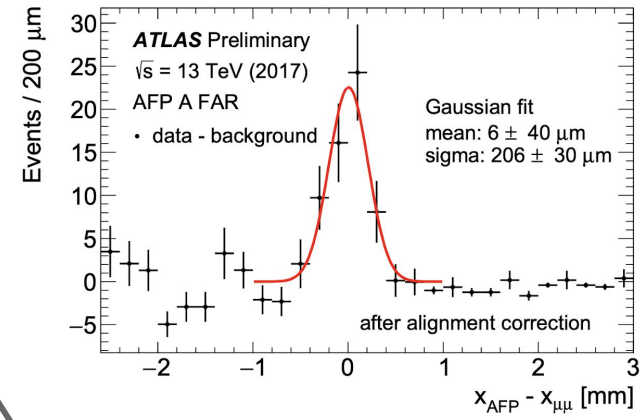

$$\xi^{\pm}_{\ell\ell} = (m_{\ell\ell}/\sqrt{s})e^{\pm y_{\ell\ell}}$$

Expected proton energy loss constrained by dimuon system

Background: no correlation (pileup)

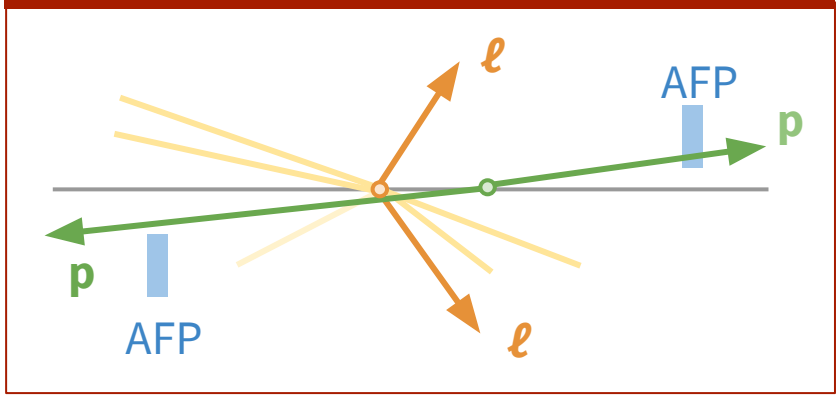

Signal: if $x_{AFP} = x_{\ell\ell}$ ⇒ aligned & calibrated

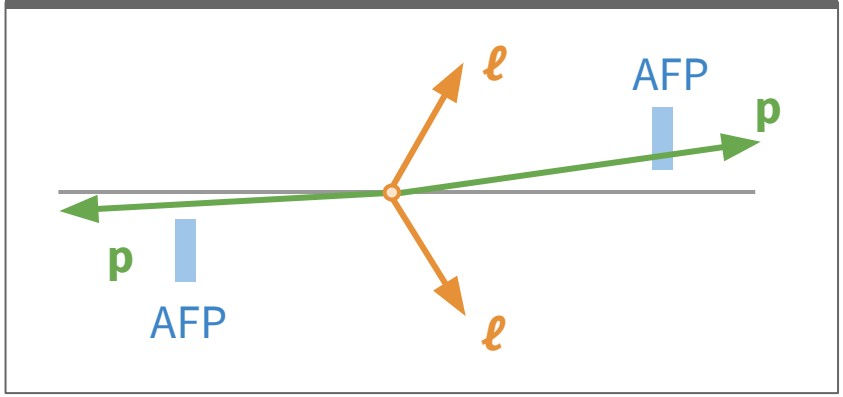

AFP acceptance

Near station acceptance "turn-on" due to e.g. edge effects plateaus at $\xi \gtrsim 0.035$

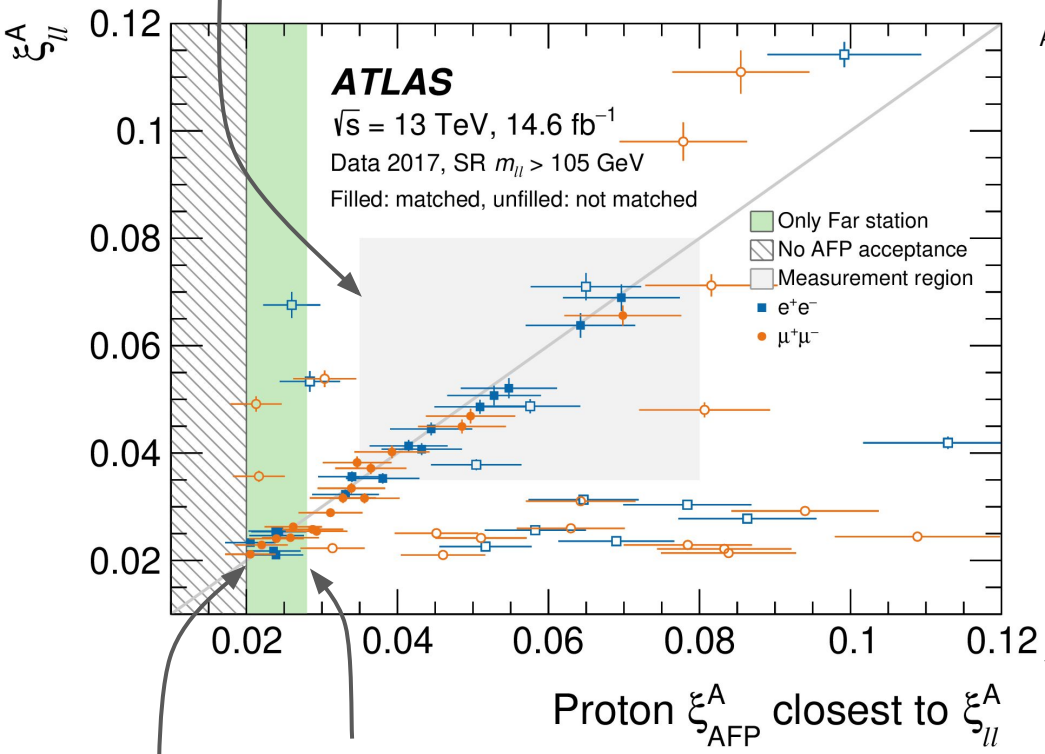

ATLAS [2009.14537]

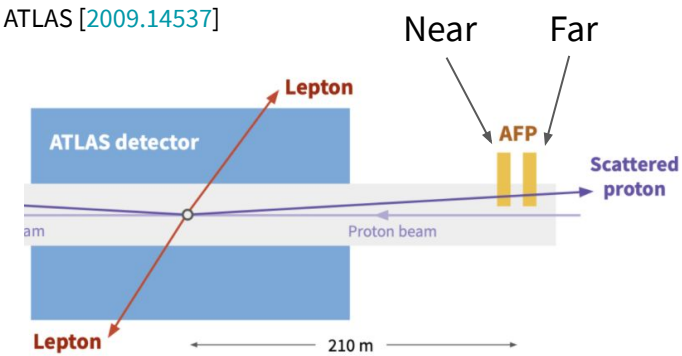

Near station acceptance switches on at $\xi \gtrsim 0.026$

Far station acceptance plateaus at $\xi \gtrsim 0.02$ bounded by beam–detector distance

Upper $\xi \lesssim 0.12$ bounded by beam collimators

[Side C is very similar]

Data/prediction comparisons

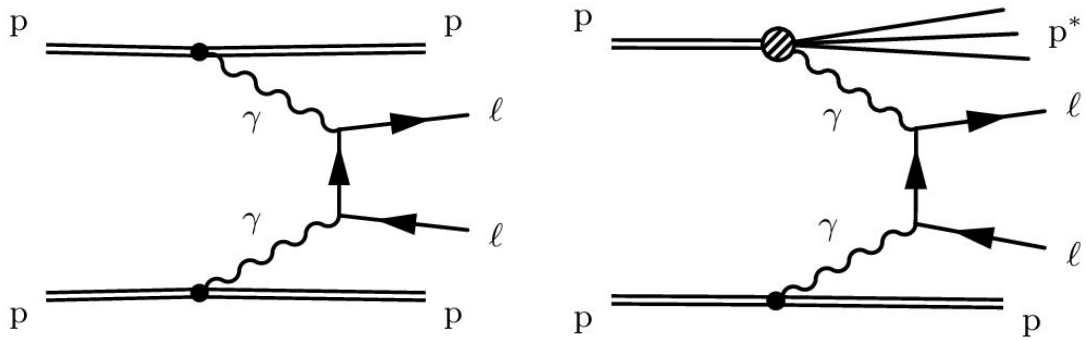

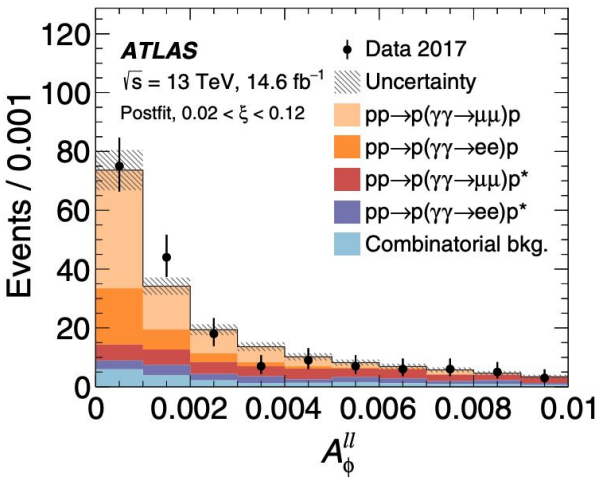

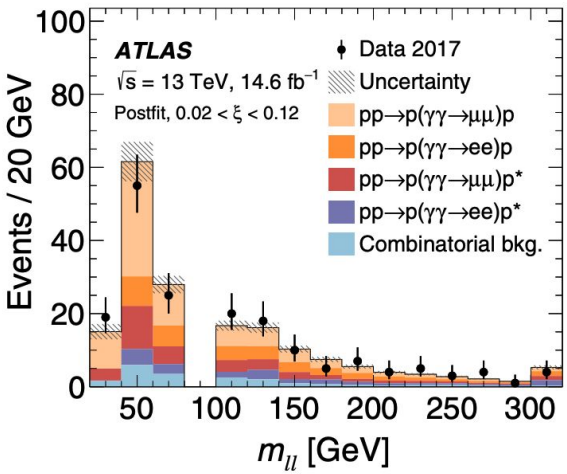

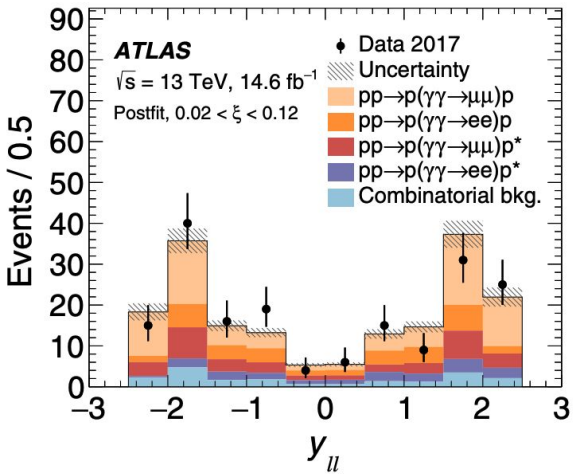

Phys. Rev. Lett. 125 (2020) 261801 [figures]

Data/prediction kinematic distributions ee/μμ

ee

μμ

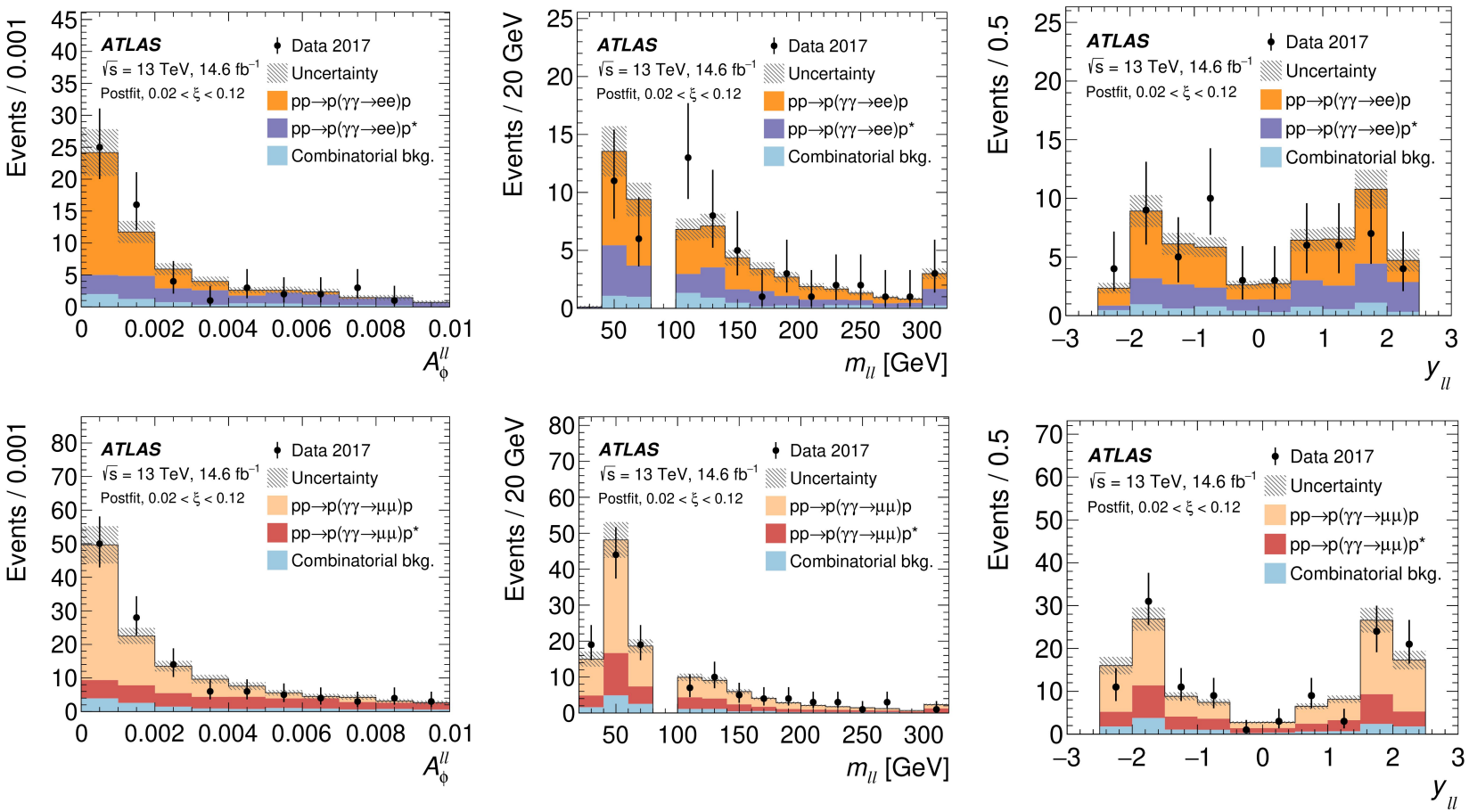

Phys. Rev. Lett. 125 (2020) 261801 [figures]

Signal vs background discrimination on Z peak

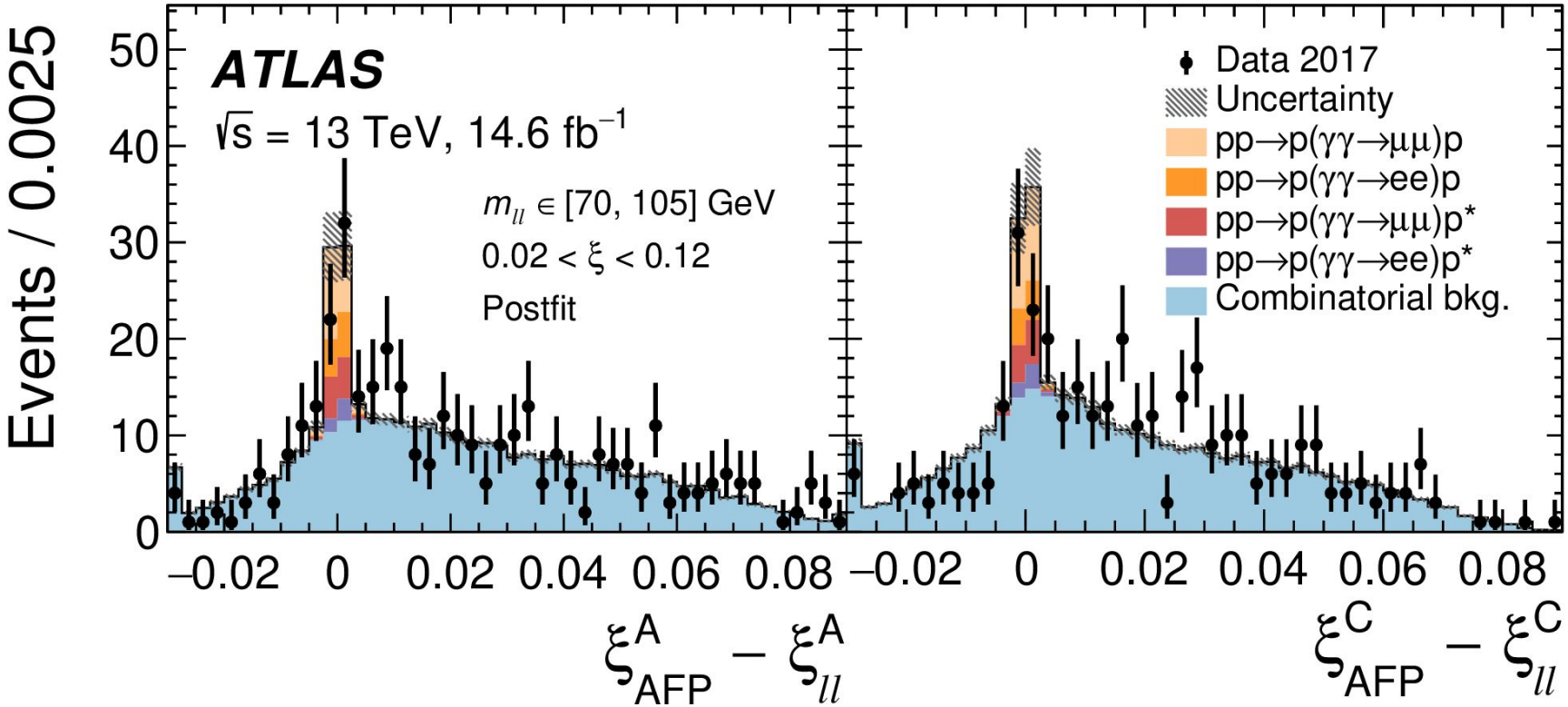

Phys. Rev. Lett. 125 (2020) 261801 [figures]

Proton energy resolution

Phys. Rev. Lett. 125 (2020) 261801 [figures]

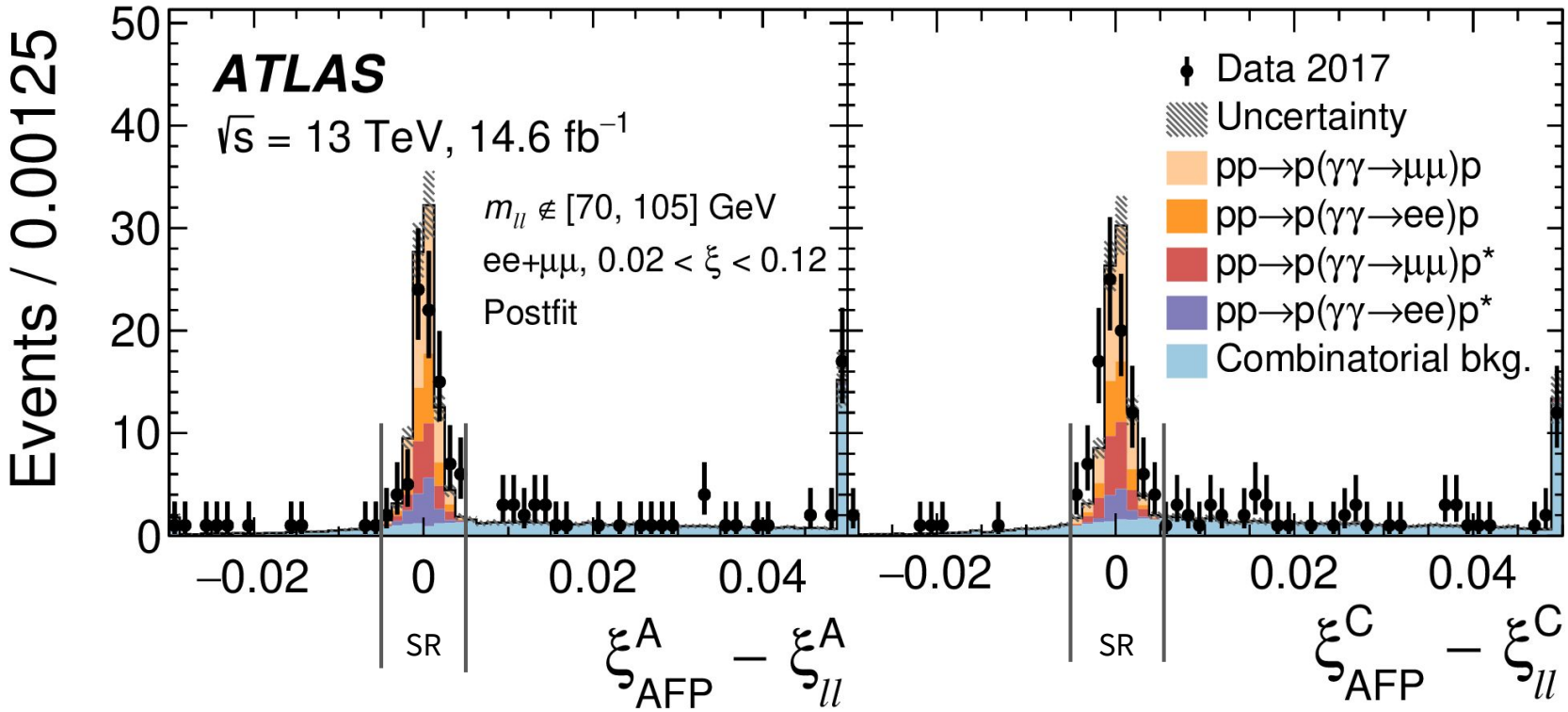

Full width at half maximum ~ 0.005 ⇒ proton energy resolution better than ~ 10%
Good resolution enables **95% signal acceptance** for **85% background rejection**
Detailed studies/more statistics to precisely quantify but first look in situ & early days

Previous differential measurements

ATLAS [1708.04053]

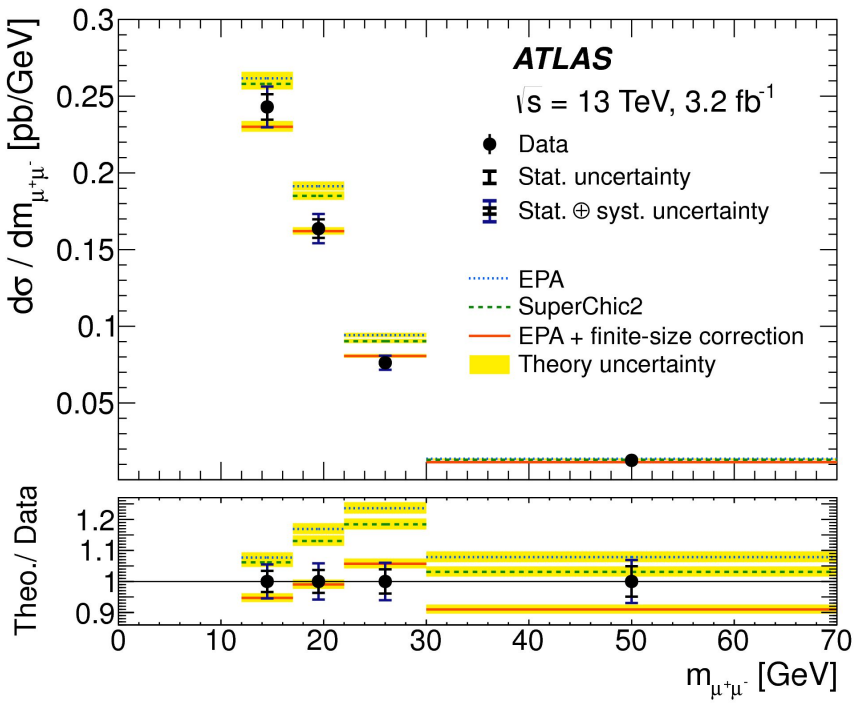

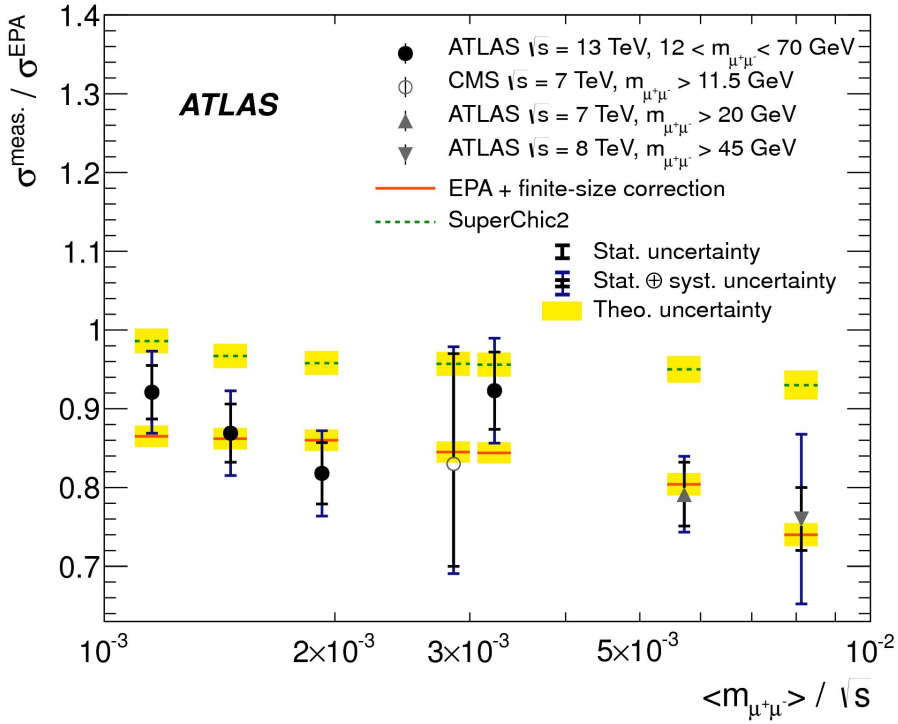

In situ dimuon calibration: systematic uncertainties

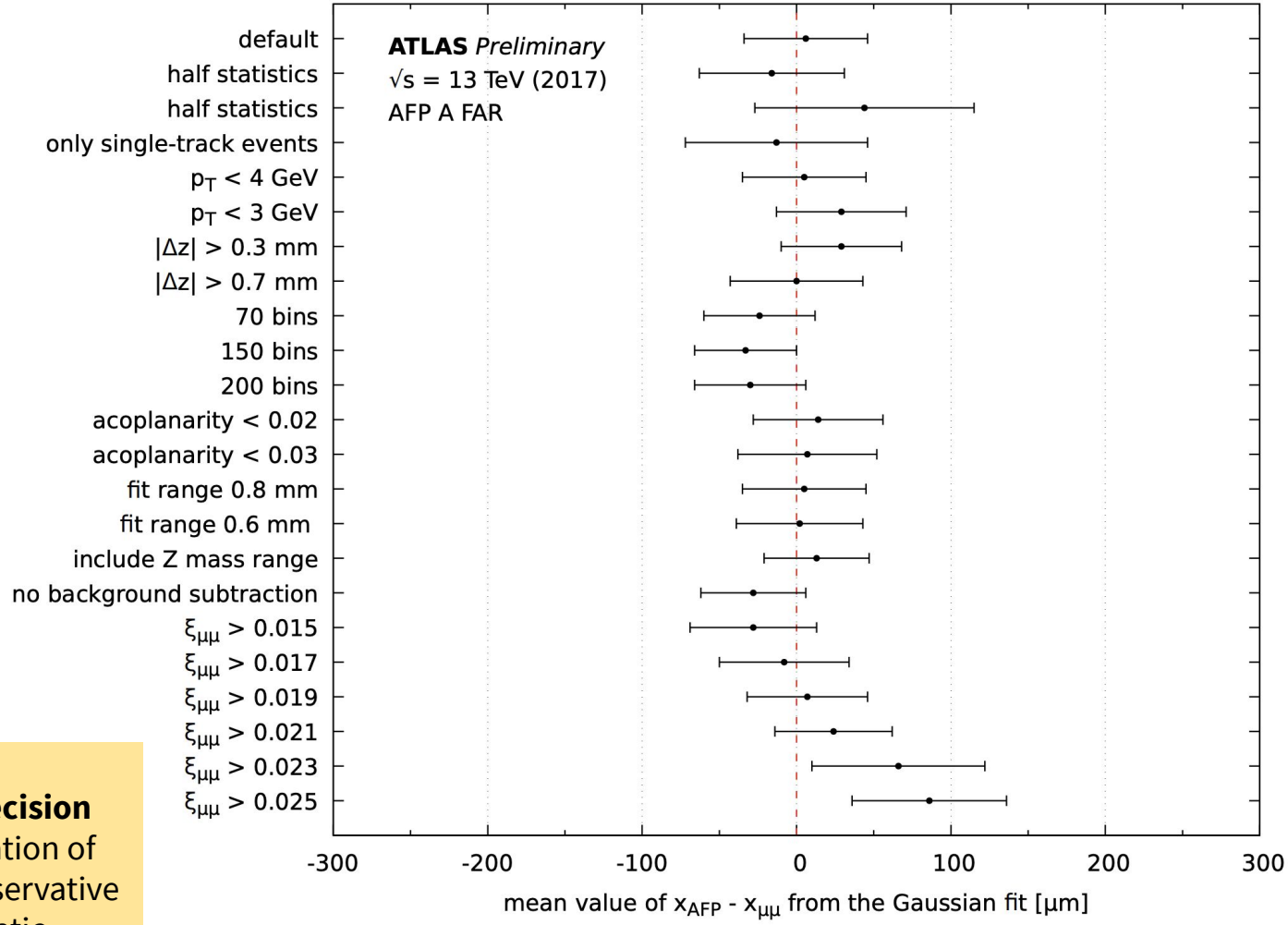

The road towards precision
Comprehensive evaluation of variations for initial conservative 300 micron systematic

Local interplane alignment

Proton leaves clusters measured at *x* position relative to plane edge

Ideal alignment

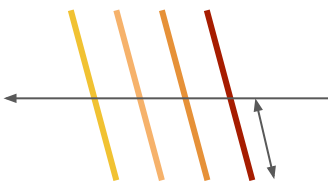

Cluster to edge distance is the same for all planes

In reality

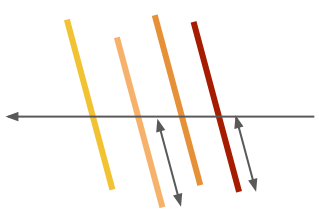

Cluster positions relative to plane edge can be different before interplane alignment

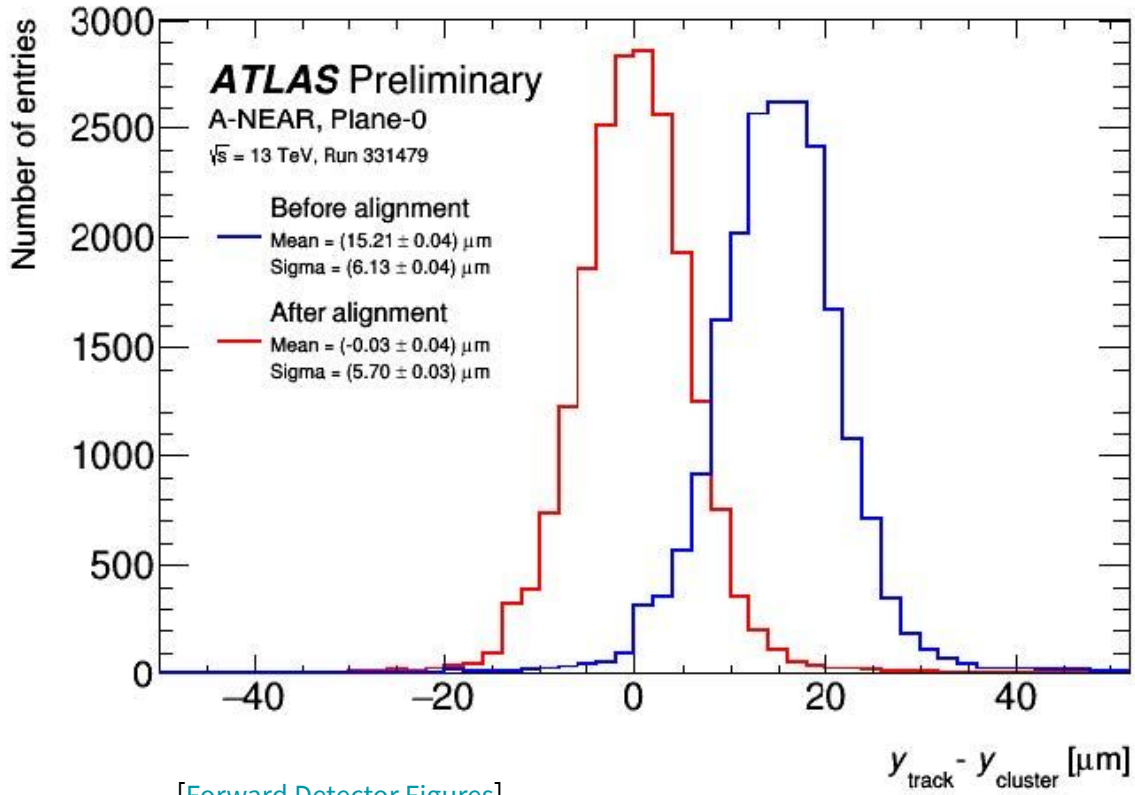

[Forward Detector Figures]

Systematic uncertainties: impact on cross-section

Source of systematic uncertainty	Impact
Forward detector	
Global alignment	6%
Beam optics	5%
Resolution and kinematic matching	3–5%
Track reconstruction efficiency	3%
Alignment rotation	1%
Clustering and track-finding procedure	$< 1\%$
Central detector	
Track veto efficiency	5%
Pileup modeling	2–3%
Muon scale and resolution	3%
Muon trigger, isolation, reconstruction efficiencies	1%
Electron trigger, isolation, reconstruction efficiencies	1%
Electron scale and resolution	1%
Background modeling	2%
Luminosity	2%

AFP systematics evaluated for first time in an analysis

pp vertices distributed as Gaussian with width σ_z

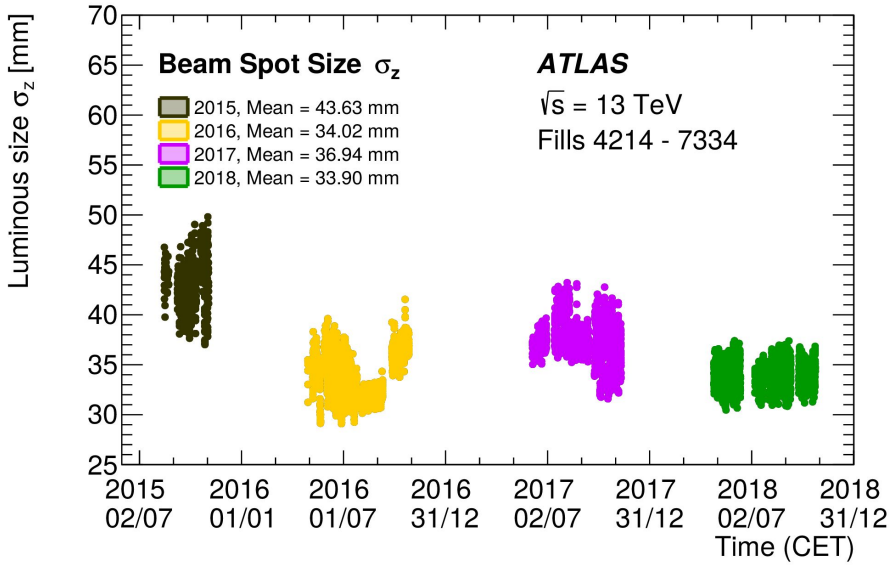

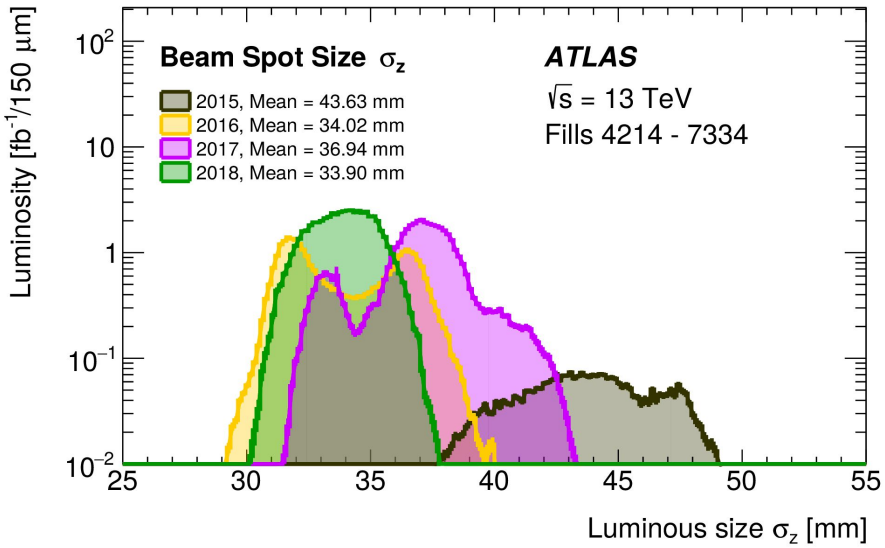

ATLAS [2010.04019]

Data driven dissociation scale factor from γγ → ℓℓ

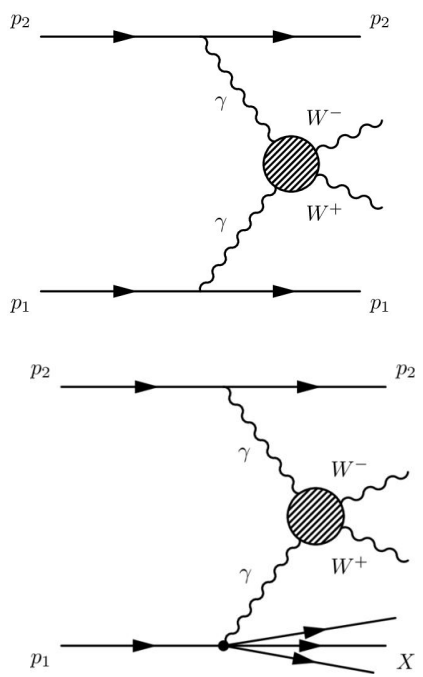

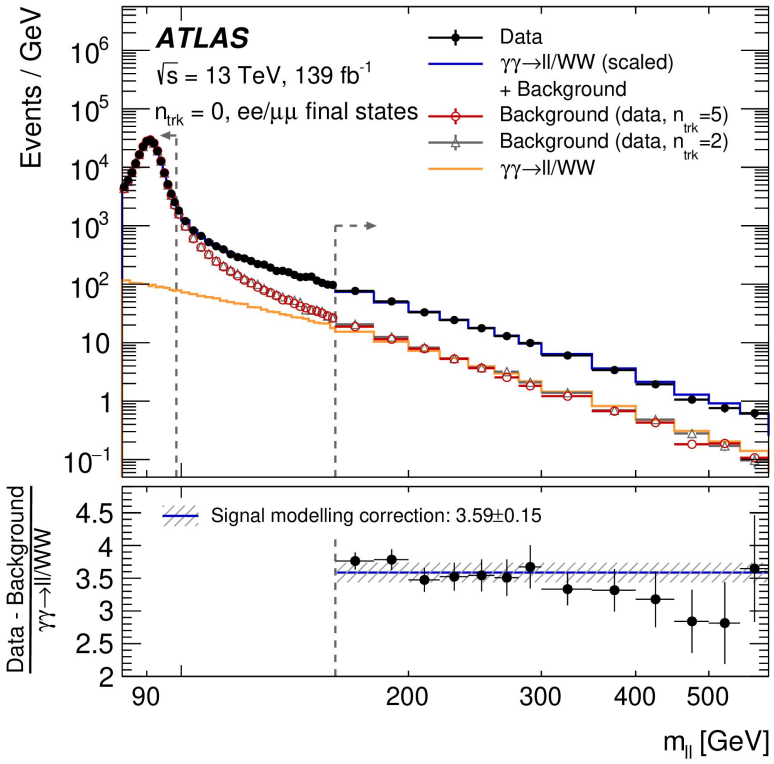

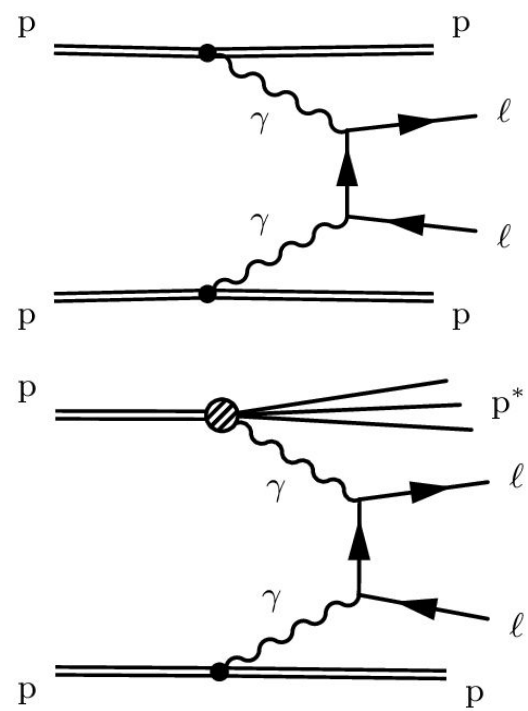

ATLAS [2010.04019]

N(track) veto efficiency vs pileup

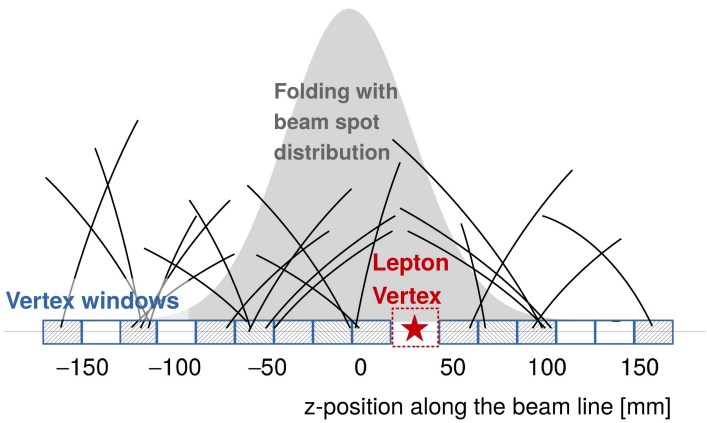

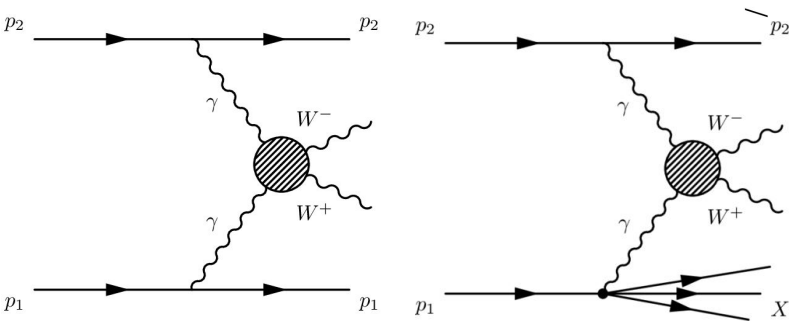

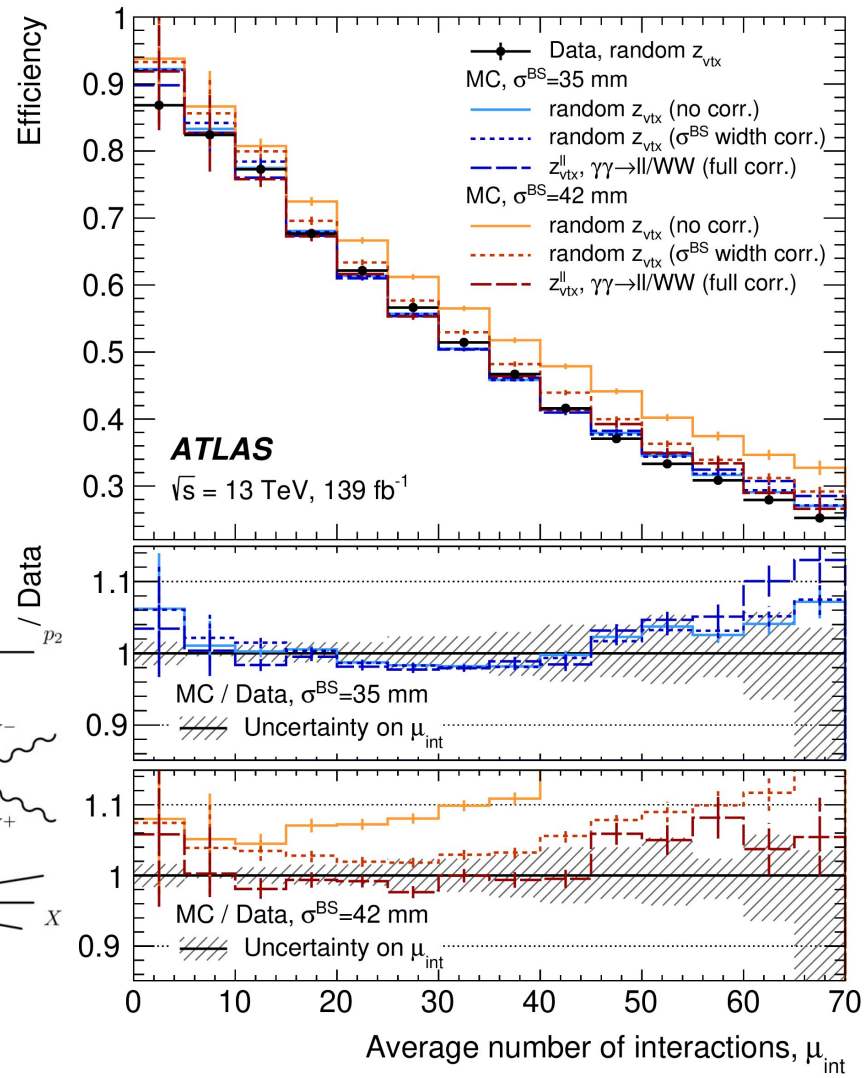

ATLAS [2010.04019]

Full Run 2 dilepton distributions from γγ → WW

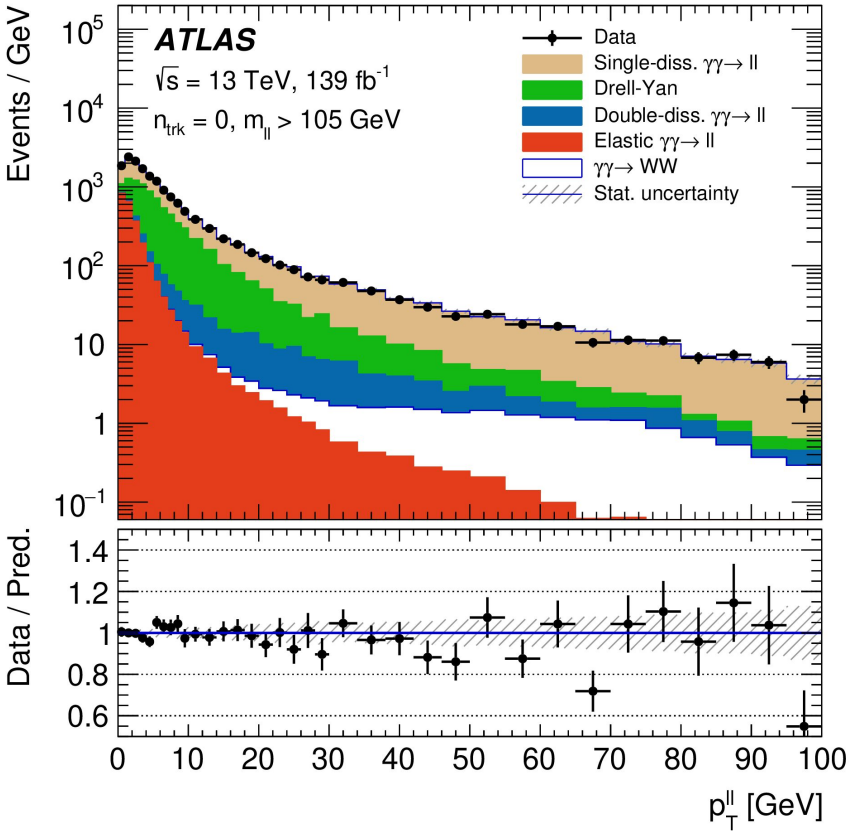

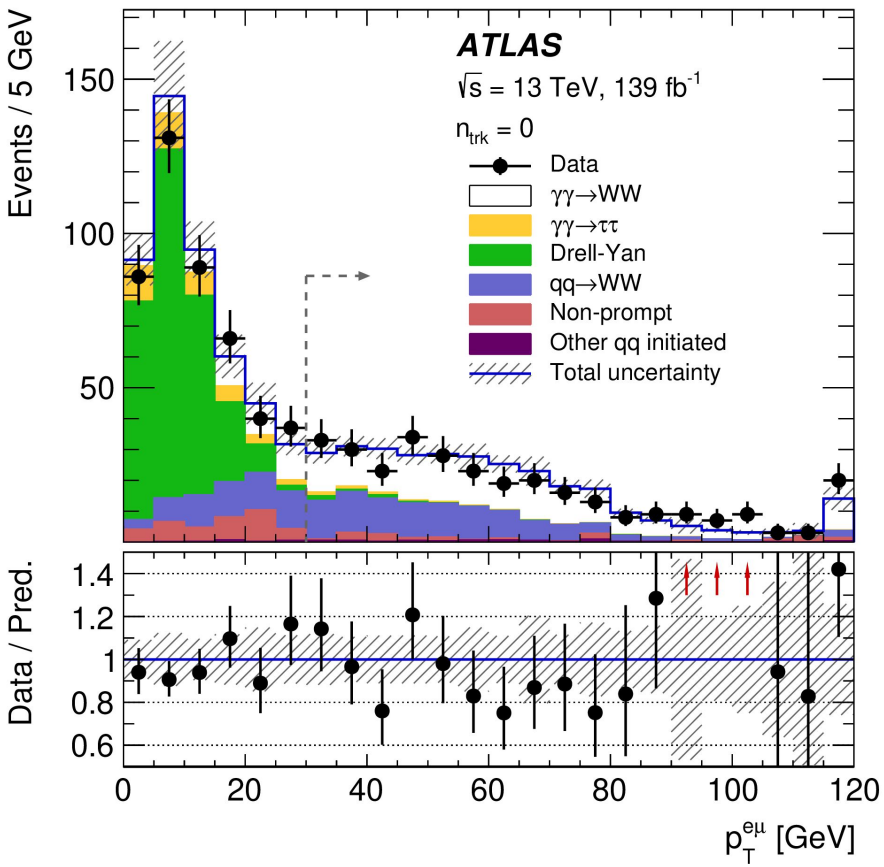

ATLAS [2010.04019]

Why this is interesting: full p_{miss} 4-vector measurable

Dream

$$\begin{pmatrix} E \\ p_x \\ p_y \\ p_z \end{pmatrix}_{\text{miss}} \Rightarrow (2m_\chi)^2$$

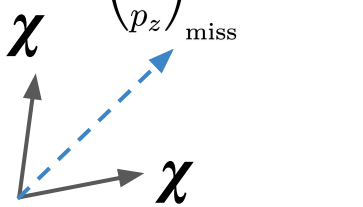

Reality

$$\begin{pmatrix} p_x \\ p_y \end{pmatrix}_{\text{miss}}$$ 2-vector

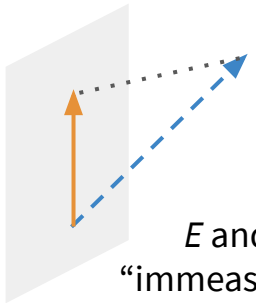

E and p_z "immeasurable"

Without AFP: only 2-vector measurable

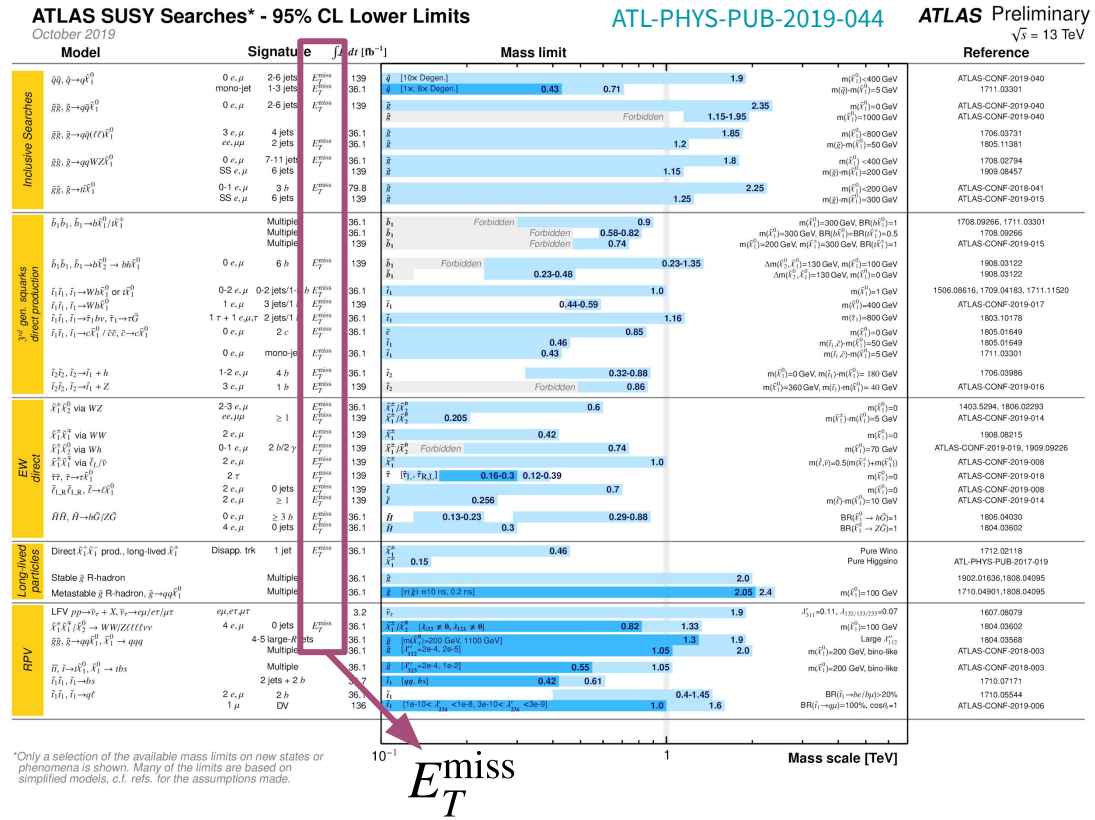

With AFP: impossible no more

$$p_{\text{miss}} = \sum_{\text{initial}} p_i - \sum_{\text{final}} p_f^{\text{visible}} \Rightarrow m^2_{\text{miss}} = p^2_{\text{miss}}$$

Enables direct dark matter mass measurement

Requires efficient time-of-flight for AFP pp vertex reconstruction (Run 3)

Near future: p_{miss} 4-vector for dark matter searches?

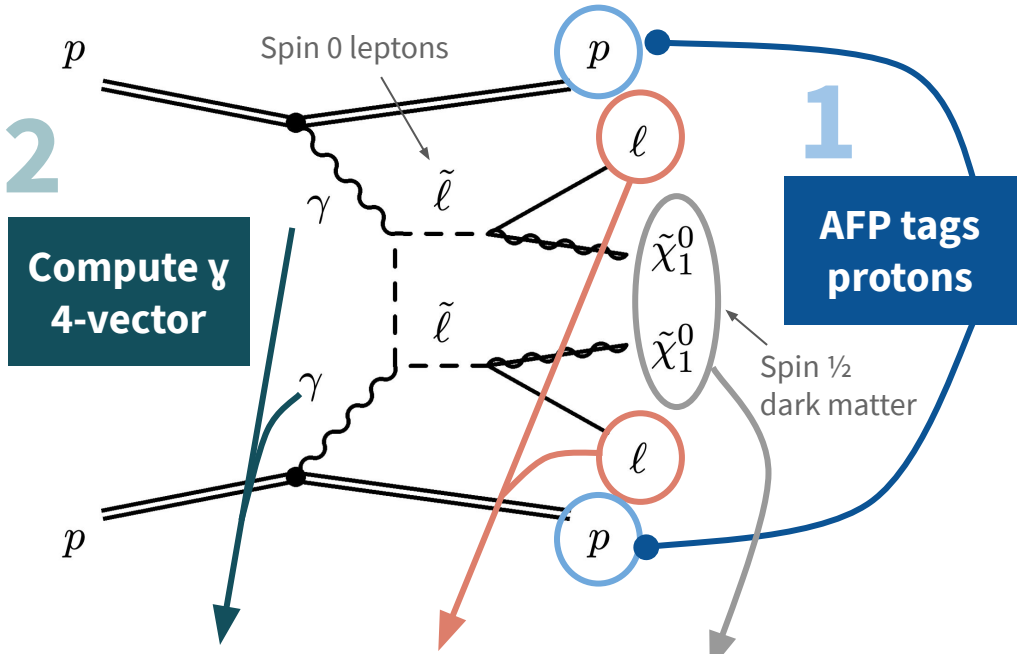

2

Compute γγ 4-vector

1

AFP tags protons

$$p_{miss} = \sum_{initial} p_i - \sum_{final} p_f^{visible} \Rightarrow m^2_{miss} = p^2_{miss}$$

3

Impossible @ pp colliders *no more*

Square 4-vector to measure DM mass

ATLAS [2010.04019]

γγ → WW just observed

Sharp threshold at 2 × m_{DM}

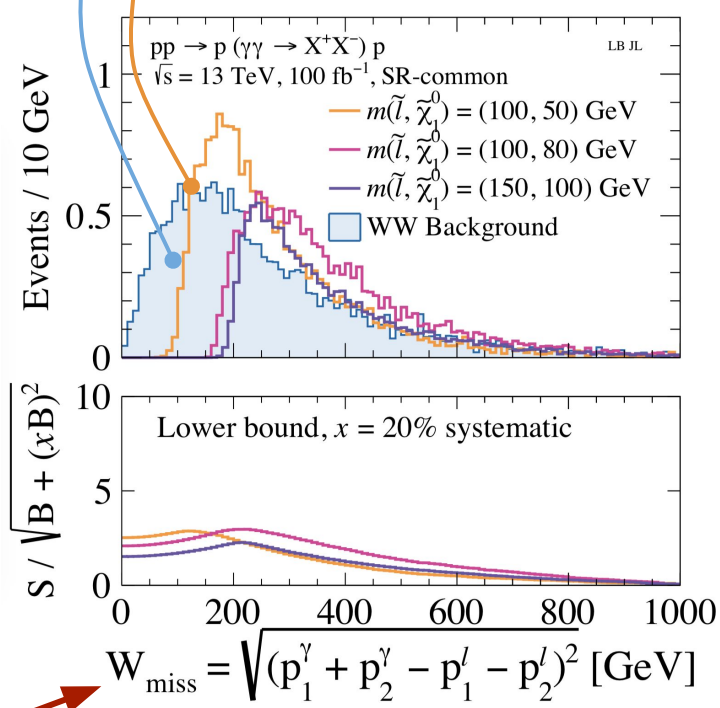

Run 3: rich physics enabled by ~10x good quality data with efficient time-of-flight

Beresford & JL [1811.06465], Harland-Lang, Khoze, Ryskin & Tasevsky [1812.04886]

Time-of-flight enables AFP pp vertex reconstruction

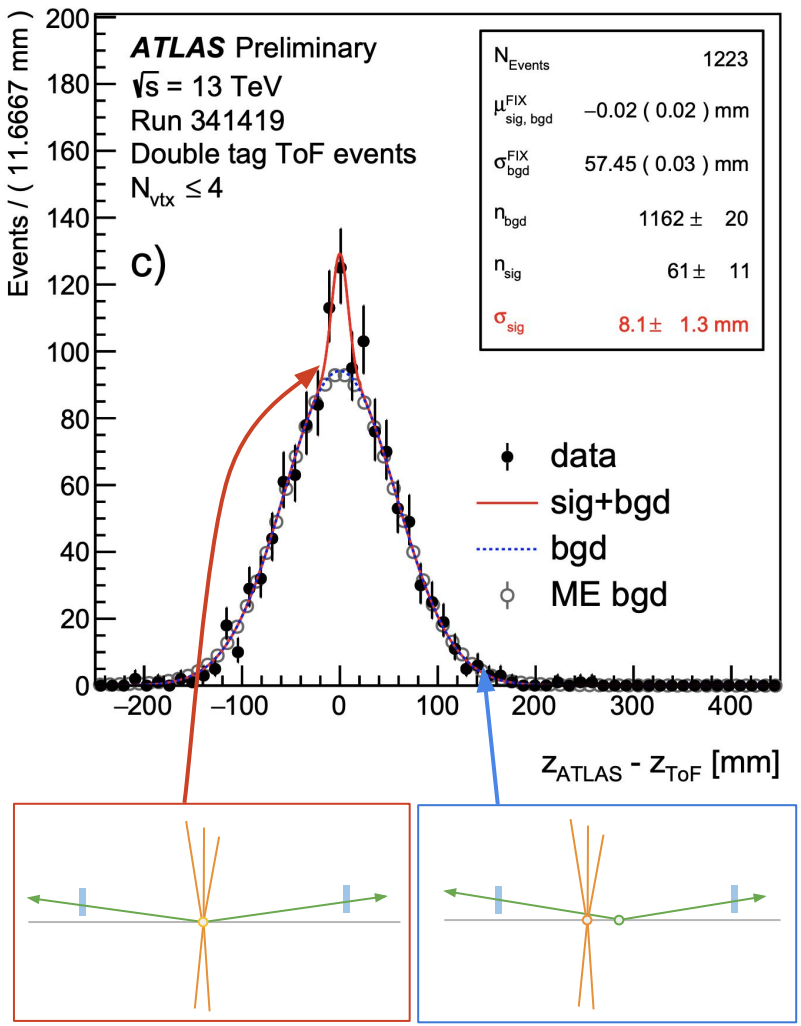

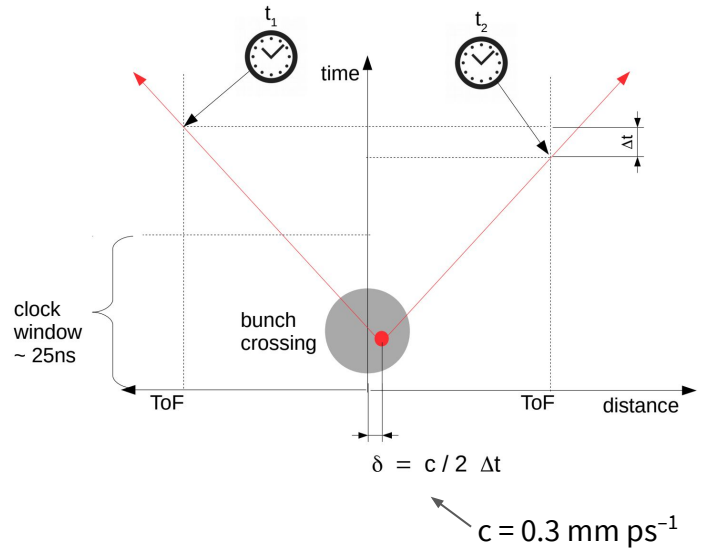

AFP deployed state-of-the-art time-of-flight
Demonstrated in situ using μ ~ 2 LHC collisions

Measured time resolution: 20 ± 4 ps (A) 26 ± 5 ps (C)
Measured pp vertex resolution: 5 ± 1 mm

Improvements ongoing for Run 3 data taking
Long-lifetime PMTs to ensure higher efficiencies

K Cerny PoS 373 Vertex2019 (2020) 055
ATL-FWD-PUB-2021-002 **[NEW!]**
More about timing in talk by Tommaso Isidori

Double-tagged ToF-ATLAS matching for different vertex cuts

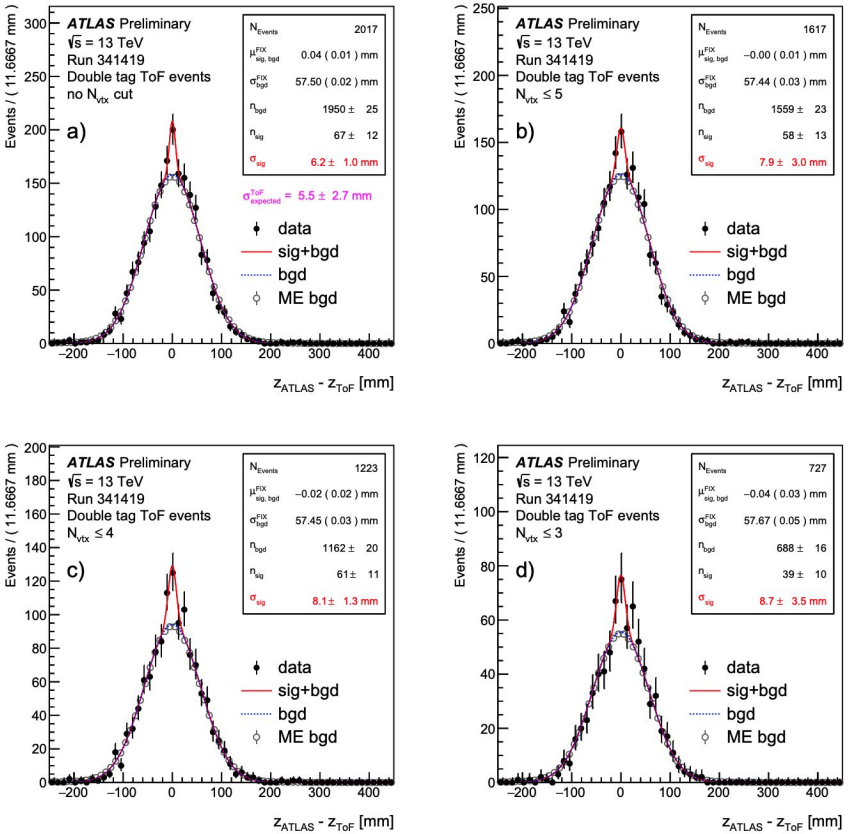

ATL-FWD-PUB-2021-002

Figure 14: The distributions of $z_{\mathrm{ATLAS}} - z_{\mathrm{ToF}}$ measured in events with ToF signals on both sides of the interaction region in run 341419, where z_{ATLAS} stands for vertex z-positions reconstructed as primary ones by ATLAS. The distributions shown in figures a)-d) correspond to ATLAS data containing a reconstructed primary vertex together with coincidence of signals in both ToF detectors in four cut scenarios with respect to number of vertices reconstructed by ATLAS, no N_{vtx} cut, $N_{\mathrm{vtx}} \leq 5$, $N_{\mathrm{vtx}} \leq 4$ and $N_{\mathrm{vtx}} \leq 3$, respectively. A double Gaussian function representing the signal and background components is fitted to unbinned data samples using the extended negative log-likelihood fit as implemented in RooFit in all N_{vtx} cut scenarios. The mean of the signal component as well as the mean and width of the background component are always estimated from a Gaussian fit to the mixed event data in each N_{vtx} cut scenario separately, denoted as $\mu_{\mathrm{sig}}^{\mathrm{FIX}}$, $\mu_{\mathrm{bgd}}^{\mathrm{FIX}}$ and $\sigma_{\mathrm{bgd}}^{\mathrm{FIX}}$. The mixed event data $z_{\mathrm{ATLAS}} - z_{\mathrm{ToF}}$ distributions are obtained by random mixing of times measured by ToF in either station and the z_{ATLAS} values which do not originate in the same collision event. The expected resolution of the ToF detector, quoted as $\sigma_{\mathrm{expected}}^{\mathrm{ToF}}$ is obtained from the known single-channel resolutions convoluted with the actual channel-hit-patterns observed in the data in the no N_{vtx} cut scenario.